ASSESSMENT OF THE IMPACT OF AWARENESS PROGRAMS ON THE TRANSMISSION DYNAMICS OF COVID-19

By

Maame Akua Korsah

Jin Wang
Professor of Mathematics
(Major Advisor)

Roger Nichols
Associate Professor of Mathematics
(Committee Member)

Lani Gao
Associate Professor of Statistics
(Committee Member)

Lakmali Weerasena
Assistant Professor of Mathematics
(Committee Member)

ASSESSMENT OF THE IMPACT OF AWARENESS PROGRAMS ON THE TRANSMISSION DYNAMICS OF COVID-19

By

Maame Akua Korsah

A Thesis Submitted to the University of
Tennessee at Chattanooga in Partial
Fulfillment of the Requirements of the Degree
of Master of Science: Mathematics

The University of Tennessee at Chattanooga
Chattanooga, Tennessee

May 2021

ABSTRACT

COVID-19, since its discovery in 2019, has posed a major health problem in the world. It is caused by the SARS-CoV-2 virus and is transmitted via infected respiratory droplets and contaminated surfaces. There is an urgent need to understand the transmission characteristics of the virus in response to social interventions. This is important to evaluate the overall impact of such programs in the management of the disease. We seek to develop a mathematical model that characterizes the transmission dynamics of COVID-19. The model analyzes the impact of preventive practices on the spread of SARS-CoV-2 by incorporating human behavior in modeling disease prevalence depending on contact rates for direct and indirect transmissions and infectious host shedding. The model is also applied to reported data from Wuhan and the state of Tennessee. Our results imply that applying strategically created awareness programs to a geological setting can eradicate COVID-19.

TABLE OF CONTENTS

LIST OF TABLES

LIST OF FIGURES

CHAPTER 1

INTRODUCTION

1.1 BACKGROUND

At present, the world faces a pandemic brought about by the SARS-CoV-2 virus. The severe acute respiratory syndrome coronavirus 2 (SARS-CoV-2), a spike protein virus is the causative agent of the widespread coronavirus disease. It is known to belong to a broad family of viruses known as the coronaviruses. The first severe illness caused by a coronavirus is the 2003 Severe Acute Respiratory Syndrome (SARS) pandemic which started in China. A second flare-up was the Middle East Respiratory Syndrome (MERS) which was discovered in 2012 in Saudi Arabia [1].The coronavirus disease 2019 was first declared a Public Health Emergency of International Concerns by the World Health Organization on January 30, 2020 [2] and finally a pandemic on March 11, 2020 [1] since the disease was determined to be a public health risk to all nations through the international spread of diseases. The disease is mostly transmitted through contact with infected respiratory droplets from coughs, sneezes and speech[3, 4]. Further research has shown that the disease could be transmitted via airborne transmission [5]. Contact with contaminated surfaces is also a known risk of infection. Some confirmed symptoms of COVID-19 known to appear after 2-14 days of exposure are coughs, fever, windedness, muscle pain, loss of smell, diarrhea sore throat, fatigue and running nose.

As at January 11, 2021 there were 680,908 new infected cases recorded worldwide with 222,921 cases in the USA, 4,255 cases in the state of Tennessee and 134 cases in China [6, 7]. A total of 11,416 deaths were recorded worldwide [6]. The American continent currently has over 40million confirmed cases with the USA leading all other countries in this region and the world with about 25million confirmed cases. While there seem to be a rapidly increasing number confirmed cases, there are also several intervention programs created to combat the current characteristics of the disease. These programs include the current vaccination programs

which begun in the last quarter of 2020 [8] , use of disinfectants, social distancing, public health education, use of nose masks and other protective shields, isolation of infected/exposed persons, funding of COVID-19 projects etc.

Awareness programs as defined in this project comprises all actions and measures aimed at the prevention and treatment of COVID-19. These range from individual behavioral change to organizational and worldwide interventions. Social distancing is one of the most utilized COVID-19 preventive strategies. It is observed by limiting face-to-face interactions by remaining in any event 6 feet from others and maintaining a strategic distance from swarmed places. This intervention has resulted in the lockdown of several countries and the closing of organizations such as schools, churches and businesses. Though these interventions appear to be drastic as they have negative impact on productivity, virtual alternatives for social gatherings, meet-ups and workplaces have been discovered. Thus, resulting in the booming economies of the virtual networking industry. Vaccinations is another ongoing major preventive strategy. Presently, 86,452,579 doses of the various vaccines have been administered worldwide with US administering about 32% of the doses.[9] Below are the vaccines currently available with their efficiencies and approvals discussed.

- The Pfizer/BioNtech vaccine is one of the popular administered vaccines known for its high efficiency against the SARS CoV-2 virus which is 95%. It was approved for emergency use in USA, UK, Canada and the EU in December 2020. Storage and transportation of the vaccine requires a temperature of -70^{o}C.[10]

- Moderna- this vaccine like the Pfizer vaccine has a high efficacy rate of 94.1% as they both use a new vaccine approach involving a messenger RNA. It has been approved for use in the USA, Canada, UK and the EU. Vaccine can be stored at 2-8^{o}C. [9]

- AstraZeneca/Oxford vaccine was approved in India on January 2, 2021 and the UK on Dec 30, 2020 for emergency use. With clinical trial size of 65,000 people, results show that the vaccine is 70% effective at preventing laboratory confirmed COVID-19.[8, 11]

- The Novavax vaccine trials currently show 89.3% efficacy against the SARS CoV-2 virus.

Initial trial phases were conducted in South Africa and the UK whiles further trials are been conducted in the USA and Mexico. This vaccine is yet to receive approvals as it is in its trial stage. [9]

- The Johnson & Johnson vaccine is the easiest to store and transport as it requires standard refrigeration out of the leading vaccines. The single-dose vaccine's efficacy rate has currently dropped from 72% in the United States to 66% in Latin America and 57% in South Africa, where a profoundly infectious variation is driving most cases. The vaccine is yet to receive approvals as it is presently in its trial stage. [12]

- Sinovac Biotech vaccine is the least effective vaccine with trial-based efficacy rate of 50.38% in Brazil. Though it has a low efficacy rate, it has been approved in Indonesia and Turkey where is known to have higher efficacy rates of 65.3% and 91.25% respectively. Vaccination requires two doses whiles storage and transportation can be done in standard refrigeration conditions. [9, 11]

- Sinopharm- it was approved in China on Dec 31st, 2020 for general use. Clinical trials conducted on the vaccine shows 79% efficiency. It is currently been administered in Morocco, China, Hungary and the United Arab Emirates.[9, 11]

- The CanSino Biologics' vaccine utilizes an innocuous cold virus to transfer its genetic payload. Only a shot of the vaccine is required. Though its efficacy is yet to be determined due to delay in clinical trials, it was cleared in June 29, 2020 for China military use as it was the first COVID-19 vaccine to enter clinical trials.[9]

Notable side effects of these vaccines are pain at the injection site, tiredness, headache, fever and chills.

1.2 PROBLEM STATEMENT

The 2019 coronavirus disease is a current health problem which was first discovered in Wuhan, China. Due to its high mortality and infection rates, and the lack of potent treatment available, it has claimed over 2.6million lives with over 118million infected cases worldwide.

Since its emergence, there has been a rise on intervention programs created with the aim of mitigating its transmission. However the extent of impact of these intervention programs is unknown. To date, there is no mathematical model that predicts the efficiency of these programs. So, the impact of the awareness programs is hard to analyze especially on a global scale. Thus, there is an urgent need for a fit-for-purpose model to probe into the impact of these awareness programs.

1.3 OBJECTIVES

The study was designed to achieve the following;

- To formulate a mathematical model that measures the impact of current awareness programs created in efforts of minimizing the spread of COVID-19.
- Analyze the stability of the model developed at the Disease-Free Equilibrium and Endemic Equilibrium.
- To develop a model to accurately predict the spread of COVID-19.
- Investigate and predict the transmission dynamics of COVID-19 in Wuhan, China and the state of Tennessee.

1.4 THESIS LAY OUT

Chapter one of the study gives a detailed background of the study, the problem statement, objectives, and thesis lay out. In Chapter 2, we shall put a pertinent related literature on COVID-19 and the SEIR models. These include publications, journals and seminars. Chapter 3 discusses the model description, model analysis and equilibrium analysis of the model. Chapter 4 is devoted to numerical simulations and results. Chapter 5, the final chapter presents the discussion of the results, conclusions, and recommendations for further studies.

CHAPTER 2

LITERATURE REVIEW

Coronavirinaea, the scientific name of the coronaviruses is a subfamily of enveloped positive-sense-single stranded RNA viruses known to infect mammals and birds[13, 14] .They usually cause infectious bronchitis and enteritis in birds, while they cause diarrhea in cows, rabbits and other mammals alike with a high mortality rate in rabbits. In humans, these viruses are responsible for several respiratory diseases [13]. Seven strains of the coronaviruses are known to have infected the human populace[14, 15]. The viruses include;

1. Human Coronavirus OC43 (HCoV-OC43)
2. Human Coronavirus HKU1 (HCoV-HKU1)
3. Human Coronavirus HKU1 (HCoV-NL63) which is also known the New Haven Coronavirus
4. Human Coronavirus HKU1 (HCoV-229E)
5. Middle East Respiratory Syndrome-related Corona Virus (MERS-CoV)
6. Severe Acute Respiratory Syndrome
7. Severe Acute Respiratory Syndrome Corona Virus 2 (COVID-19)

Other than the current COVID-19 vaccines, there are no other antiviral treatment to prevent or cure infections caused by the coronaviruses[16]. Thus there is the need to measure the impact of the current measures put in place to eradicate the coronavirus disease 2019.

Mathematical modeling has become an increasingly important area as computers are expanding our innate ability in translating mathematical equations and formulations into precise conclusions. These models by using basic assumptions and collected statistics can project and

predict the progress of infectious diseases, show the likelihood of an epidemic, and aid in deciding which interventions are required.

This chapter focuses on the various studies done in attempt to model the epidemiology of the coronavirus disease 2019. Several researches have been conducted to aid in the understanding of the intrinsic bacterial behavior and transmission dynamics of the causative agents of COVID-19. However, none has investigated the impact of the intervention programs using a COVID-19 SEIR deterministic model with compartments for awareness programs and virus concentration despite the vaccination and preventive measures we have today.

A deterministic model also known as compartmental model, describes the transportation of materials in a system consisting of a collection of groups that are connected by material flow. Each compartment comprises of characterized materials and can exchange these materials with other compartments following some strict principles set for each compartment. The compartments are assumed to be homogeneous entities within which the materials being modelled are equivalent. Materials can also move into a compartment from outside through a source and be removed to the outside of the biological system under study through a sink or drain. [17]
Deterministic models help to account for the movement of material under study by following some conservational laws. In the deterministic model, the compartments are developed based on the law of conservation of energy which states that energy cannot be created nor destroyed but can change from one form to another. Thus, the differences in energy from one compartment to another can be calculated since no energy is lost during the exchange of materials.
Most deterministic models, in mathematical epidemiology have more than one compartment represented as equations. These models are generated by following the conservational law of energy for each equation. Before proposing a model for the transmission behavior of COVID-19, we briefly examine the earlier proposed models for the study of COVID-19 and their results. We also in this chapter assess the basic SEIR model and the various ways it has been modified in disease modelling.

2.1 THE SEIR MODEL

In 1927, Kermack and McKendrick in their paper "A contribution to the Mathematical Theory of Epidemics" introduced the idea of having a general procedure to analyze the spread of contagious epidemics. [18] This general procedure is known today as the SIR model. In the basic SIR framework, the groups or compartments considered are identified as S-susceptible, I-infected and R-removed. The process of disease modelling begins with an interaction between an infected individual and a group of individuals who are at risk of being infected. Several susceptible people will then become infected, thus joining the infected group. An infected person then either dies or recovers from the disease. In both cases they are removed from the infected compartment. When there is an epidemic, the number of susceptible people decreases as it acts on a brief timeframe and might be portrayed as a sudden outbreak of a disease infecting a substantial portion of the populace in a geological area before disappearing. In an endemic situation, however, the disease becomes established in the population and remains for an extended time.[19]

In constructing epidemics models, demographic effects such are ignored due to the short duration of the disease since demographic time scales are ordinarily much longer than the disease timeframe; thus, they are dismissed. Then again, since endemics may endure for a longer time, it becomes important to include demographic effects in endemic models.[19]
The SEIR model is a modified SIR model which characterizes the incubation period between the infected period (entry of pathogen) and the stage of infectiousness (shedding of pathogen). It is very important to model the incubation period (E) explicitly since the individual at the incubation period has been exposed to a pathogen that may be active or dormant. It has been used in the study of epidemiological patterns and diseases control since it was proposed by Cooke and Driessche (1996) [20, 21].

The SEIR model like the SIR model describes the progression of an epidemic considering the total population to be equally likely to get infected. Here immunity after infection is assumed, which means individuals do not return to the susceptible compartment after recovery. Kermack and McKendrick (1927) expressed an epidemic as a sudden outbreak of an infection

which spreads to several members of a geographical setting [18]. These outbreaks recur until the majority of the populace develops immunity.

The formulation of the SEIR model was one of the first breakthroughs of mathematical epidemiology. It has helped in the study of the transmission dynamics of infections such as cerebrospinal meningitis, malaria, hepatitis A and B [17, 22, 23]. For instance Turner et al (2016) in their comprehensive study of malaria in humans employed the SEIR model. Combined with a proposed SEI model for malaria in mosquitos they found the causes of the spread and growth rate of malaria in humans[22]. Side et al (2017) also considered the SEIR framework in their model simulations for Hepatitis B while considering the factors that influence the dissemination in a population [23]. Several stability analysis have also been conducted on the SEIR model[24, 25, 20, 26]. The global dynamics of the SEIR model with varying population size has been studied and found that the endemicity of a disease with non-negligible latent period includes the latent and infectious fractions of a population. Li et al (1999) also discovered three threshold parameters in their disease dissemination analysis; the modified contact number (measures the ability of a disease to become endemic), the contact number (determines the dynamics of the population) and the parameter which measures the extent that diseases regulate the growth of the host population[24]. Recently, Weinstein et al (2020) in their study of the SEIR model found the analytical solution of the model by recasting the SEIR model as a single 2nd order nonlinear ODE in ln(s)[26]. Ranjit et al (2019) also proposed and studied the SEIR model in controlling highly contagious diseases, they recommended the use of the model in related studies.[27]

COVID-19 colloquially termed as coronavirus, has a fast-spread dissemination rate which has the attention of all and as such many have conducted studies to understand its dynamics. Mathematical epidemiology has played a major role in the research done so far and several epidemiological models have been formulated and studied to predict and understand the viral replication and transmission dynamics of the SARS CoV-2 [28, 29, 30]. One of the early studies was conducted by Li et al (2020) to unravel the cause of rapid dissemination of the coronavirus disease. Their analysis was done by observing the reported data from December 2019 to January 2020 in Wuhan using a network dynamic metapopulation model. They

estimated that about 86% of all infections are undocumented with 95% confidence interval of 82-90%[30]. Thus there were some undetected individuals present in the population who had been exposed to the virus and were facilitating the spread. The same dynamics are observed in the disease's non negligible latent period. Sabbih et al (2020) proposed the SEIS model to study the disease transmission dynamics suspecting that individual who had recovered from COVID-19 were still susceptible to reinfection. They also proposed a viral replication model to help comprehend virus-host cell interactions[28]. Yang and Wang (2020) based on current clinical diagnosis on reinfection cases proposed the SEIR model in their study of the outbreak of COVID-19 in Wuhan, the epicenter of the disease. Through numerical simulation and mathematical analysis, they predicted that the coronavirus disease would persist and become epidemic [31]. Mandal et al (2020) in their investigation to identify rational intervention strategies to control the dissemination of COVID-19 in India employed the SEIR. Their analysis was limited to quarantine and airport screening as intervention programs. They recommended more intervention programs to aid in the mitigation response needed[29]. More recently, Mbogo and Odhiambo (2021) studied the impact of social distancing and mass-testing in Kenya. Their analysis was conducted using the SEIHQRD model, a modified SEIR epidemic model. Their findings also suggested that a more dedicated effort from individuals and the government was required to decrease the infection rate in Kenya[32]. Though several works have been done to understand the dynamics of the current pandemic, research on the total impact of awareness programs created is scarce.

CHAPTER 3

FORMULATION OF MODEL AND ANALYSIS

The population is partitioned into the four SEIR subgroups which consists of individuals who are S-susceptible, E-exposed, I-infected and R-recovered. The number of awareness programs M(t) and the virus concentration in the environment V(t) at a given time t is included in the model to simulate the impact of the awareness programs. The model is formulated as;

$$\begin{aligned}
\frac{dS}{dt} &= \Lambda - \beta_E(M)SE - \beta_I(M)SI - \beta_V(M)SV - \mu S + \sigma R, \\
\frac{dE}{dt} &= \beta_E(M)SE + \beta_I(M)SI + \beta_V(M)SV - (\alpha+\mu)E \\
\frac{dI}{dt} &= \alpha E - (\gamma+\omega+\mu)I, \\
\frac{dR}{dt} &= \gamma I - (\mu+\sigma)R, \\
\frac{dV}{dt} &= \xi_1(M)E + \xi_2(M)I - \rho V \\
\frac{dM}{dt} &= \chi + \eta I - \nu M
\end{aligned} \tag{3.1}$$

where S, E, I and R denote the number of susceptible, exposed, infected and recoverd individuals respectively, V is the concentration of the virus in the environment and M the number or density of valid awareness programs. All the parameters involved in the model are positive. The parameter Λ denotes the population influx, μ the natural death rate of human individuals, σ the waning rate of the disease induced immunity, α^{-1} denotes the incubation period, γ the recovery rate and ω the rate of death induced by infection.$\beta_E(M)$, $\beta_I(M)$, $\beta_V(M)$ represent the direct and indirect transmission rates by exposed persons, infected individuals and the virus respectively.

Meanwhile, $\xi_1(M)$ and $\xi_2(M)$ are host shedding rates from the exposed and infected individuals respectively and ρ is the rate at which viruses are removed from the environment.

The number of awareness programs grows with an influx of χ and it is stimulated by disease prevalence at the rate of η and decays with time at a rate of ν. We assume

1. The transmission and host shedding rates are positive functions on $[0, M_{\max}]$
2. $\beta_E'(M) \leq 0, \beta_I'(M) \leq 0,\ \beta_V'(M) \leq 0, \xi_1'(M) \leq 0$ and $\xi_2'(M) \leq 0$

where $M_{\max} = \left(\chi + \eta \frac{\Lambda}{\mu}\right) / \nu$

3.1 MODEL ANALYSIS

We begin the model analysis by finding the basic reproduction number,$\mathscr{R}_0$ using the method of next-generation matrix. The new infection matrix and transition matrix were found as follows;

$$f = \begin{pmatrix} \beta_E(M)SE + \beta_I(M)SI + \beta_V(M)SV \\ 0 \\ 0 \end{pmatrix} \quad \mathscr{V} = \begin{pmatrix} (\alpha+\mu)E \\ -\alpha E + (\gamma+\omega+\mu)I \\ -\xi_1(M)E - \xi_2(M)I + \rho V \end{pmatrix}$$

$$F = \begin{bmatrix} \beta_E(M)S & \beta_I(M)S & \beta_V(M)S \\ 0 & 0 & 0 \\ 0 & 0 & 0 \end{bmatrix} \quad V = \begin{bmatrix} (\alpha+\mu) & 0 & 0 \\ -\alpha & (\gamma+\omega+\mu) & 0 \\ -\xi_1(M) & -\xi_2(M) & \rho \end{bmatrix} \tag{3.2}$$

Clearly at the unique disease free equilibrium; DFE

$$X_0 = (S_0, E_0, I_0, R_0, V_0, M_0) = (\frac{\Lambda}{\mu}, 0, 0, 0, 0, \frac{\chi}{\nu})$$

Thus

$$\mathscr{R}_0 = \rho(FV^{-1}) = \frac{\beta_E(M_0)S_0}{(\alpha+\mu)} + \frac{\alpha\beta_I(M_0)S_0}{(\alpha+\mu)k} + \frac{(k\xi_1(M_0) + \alpha\xi_2(M_0))\beta_V(M_0)S_0}{\rho(\alpha+\mu)k}$$

Here ρ implies the spectral radius of the matrix FV^{-1} and $k = (\gamma + \omega + \mu)$

The first and second terms of $\mathscr{R}_0$; $\mathscr{R}_{0E}$ and $\mathscr{R}_{0I}$ comes from the direct transmission route which is the transmission from the exposed and infected respectively. The last term, $\mathscr{R}_{0V}$ represents the contribution from the indirect transmission route (environment to susceptible).That is;

$$\mathscr{R}_{0E} = \frac{\beta_E(M_0)S_0}{(\alpha+\mu)}$$
$$\mathscr{R}_{0I} = \frac{\alpha\beta_I(M_0)S_0}{(\alpha+\mu)k}$$
$$\mathscr{R}_{0V} = \frac{(k\xi_1(M_0)+\alpha\xi_2(M_0))\beta_V(M_0)S_0}{\rho(\alpha+\mu)k}$$

We continue by comparing the above $\mathscr{R}_0$ to the actual $\hat{\mathscr{R}}_0$ without the presence of the awareness programs, thus $M = 0$.

$$\hat{\mathscr{R}}_0 = \frac{\beta_E(0)S_0}{(\alpha+\mu)} + \frac{\alpha\beta_I(0)S_0}{(\alpha+\mu)k} + \frac{(k\xi_1(0)+\alpha\xi_2(0))\beta_V(0)S_0}{\rho(\alpha+\mu)k}$$

Based on the assumptions made above, it is observed that $\mathscr{R}_0 \leq \hat{\mathscr{R}}_0$, indicating that the awareness programs reduces disease transmission risk.

CHAPTER 4

EQUILIBRIUM ANALYSIS

Let (S, E, I, R, V, M) be an equilibrium of model (3.1), which satisfies the following equations;

$$\begin{aligned}
&\Lambda - \beta_E(M)SE - \beta_I(M)SI - \beta_V(M)SV - \mu S + \sigma R = 0,\\
&\beta_E(M)SE + \beta_I(M)SI + \beta_V(M)SV - (\alpha+\mu)E = 0,\\
&\alpha E - kI = 0,\\
&\gamma I - (\mu+\sigma)R = 0,\\
&\xi_1(M)E + \xi_2(M)I - \rho V = 0\\
&\chi + \eta I - \nu M = 0
\end{aligned} \tag{4.1}$$

which yields;

$$\begin{aligned}
S &= \frac{1}{\mu}[\Lambda - (\alpha+\mu)E + \sigma R]\\
E &= \frac{kI}{\alpha}\\
R &= \frac{\gamma I}{(\mu+\sigma)}\\
V &= \frac{k\xi_1(M) + \alpha\xi_2(M)}{\alpha\rho} I\\
M &= \frac{\chi + \eta I}{\nu}
\end{aligned} \tag{4.2}$$

It follows from $S+E+I+R = \frac{\Lambda}{\mu}$ and the second and third equations of (4.2)

$$S_1 = \frac{\Lambda}{\mu} - b_1 I = \phi(I), \tag{4.3}$$

with $b_1 = 1 + \frac{k}{\alpha} + \frac{\gamma}{(\mu+\sigma)}$

Combining equation 2 of (4.1) with (4.2) we get

$$S_2 = \psi(I) = \frac{(\alpha+\mu)}{f(I)} \tag{4.4}$$

where $f(I)$ is defined with $h(I) = M = \frac{\chi+\eta I}{\nu}$ as;

$$f(I) = \beta_E(h(I)) + \frac{\alpha}{k}\beta_I(h(I)) + \frac{k\xi_1(h(I)) + \alpha\xi_2(h(I))}{k\rho}\beta_V(h(I))$$

We now consider the curves $S = \phi(I)$ and $S = \psi(I)$, $I \geq 0$

The intersection of the curves in $\mathbb{R}^2_+$ determines the non-DFE equilibria. Note that

$$f'(I) = h'(I)\left[\beta'_E(h(I)) + \frac{\alpha}{k}\beta'_I(h(I)) + \frac{k\xi'_1(h(I)) + \alpha\xi'_2(h(I))}{k\rho}\beta_V(h(I)) + \frac{k\xi_1(h(I)) + \alpha\xi_2(h(I))}{k\rho}\beta'_V(h(I))\right]$$

Using assumptions 1 and 2, and the fact that $h'(I) = \frac{\eta}{\nu} > 0$, we see that $f'(I) \leq 0$. Which implies that $\psi(I)$ is an increasing function. On the other hand,

$$b_1 > 0 \text{ and } \phi'(I) = -b_1 < 0$$

Thus $\phi(I)$ is strictly decreasing.

Additionally, one is able to verify that at $I = 0$, $\phi(0) = \frac{\lambda}{\mu} = S_0$

$$\psi(0) = (\alpha+\mu)\left[\beta_E(\frac{\chi}{\nu}) + \frac{\alpha}{k}\beta_I(\frac{\chi}{\nu}) + \frac{k\xi_1(\frac{\chi}{\nu}) + \alpha\xi_2(\frac{\chi}{\nu})}{k\rho}\beta_V(\frac{\chi}{\nu})\right]^{-1} = \frac{S_0}{\mathscr{R}_0}$$

At $I = \frac{\Lambda}{\mu b_1}$, $\phi(\frac{\Lambda}{\mu b_1}) = 0$ and $\psi(\frac{\Lambda}{\mu b_1}) > 0$. Therefore we can conclude that;

1. If $\mathscr{R}_0 > 1$, these two curves have a unique intersection lying in the interior of $\mathbb{R}^2_+$, due to $\psi(0) < \phi(0)$ and $\psi(\frac{\Lambda}{\mu b_1}) > \phi(\frac{\Lambda}{\mu b_1})$. Moreover, at this intersection point, equation (4.2) yields $E, R, V, M > 0$ (since $I > 0$).

2. If $\mathscr{R}_0 \leq 1$, the two curves have no intersection in the interior of $\mathbb{R}^2_+$ as $\psi(0) \geq \phi(0)$.

Therefore, by Equation (4.2), we find that if $\mathscr{R}_0 \leq 1$, the model (3.1) admits a unique equilibrium, the DFE, $X_0 = (S_0, E_0, I_0, R_0, V_0, M_0)$; and it admits two equilibria, the DFE and an endemic equilibrium (EE), $X_* = (S_*, E_*, I_*, R_*, V_*, M_*)$, if $\mathscr{R}_0 > 1$.

In what follows, we perform a study on the global stability of the DFE. By a simple comparison principle, we find that $0 \leq S + E + I + R \leq S_0$,

$0 \leq V \leq \frac{(\xi_1(0)+\xi_2(0))S_0}{\rho}$ and $M_0 \leq M \leq M_{\max}$

Thus it leads to a biological feasible domain

$$\Omega = \left\{ \begin{array}{c} (S,E,I,R,V,M) \in \mathbb{R}^6_+ : S+E+I+R \leq S_0, 0 \leq V \leq \frac{(\xi_1(0)+\xi_2(0))S_0}{\rho} \\ \text{and } M_0 \leq M \leq M_{\max} \end{array} \right\}$$

Theorem 4.0.1. *The following statements hold for model (3.1)*

1. *If $\mathscr{R}_0 \leq 1$,the DFE of system (3.1) is globally assymptotically stable in Ω.*
2. *If $\mathscr{R}_0 > 1$, the DFE of system (3.1) is unstable and there exists a unique endemic equilibrium. Moreover the disease is uniformly persistent, namely, $\liminf_{t\to\infty}(E(t), I(t), V(t)) > (c,c,c)$ for some $c > 0$ with the initial condition in the interior of Ω, denoted by $\mathring{\Omega}$.*

Proof

Let $\mathbf{x} = (E, I, V)^T$ We can easily verify that

$$\frac{d\mathbf{x}}{dt} \leq (F - V)\mathbf{x}$$

where the matrices F and V are given above in equation (3.2)

Take $\mathbf{u} = \left(\beta_E(\frac{\chi}{v}), \beta_I(\frac{\chi}{v}), \beta_V(\frac{\chi}{v})\right)$. It follows from the fact that $\mathscr{R}_0 = \rho(FV^{-1}) = \rho(V^{-1}F)$ and direct calculation that $\mathbf{u}$ is a left eigenvector associated with the eigenvalue $\mathscr{R}_0$ of the $V^{-1}F$, that is $\mathbf{u}V^{-1}F = \mathscr{R}_0\mathbf{u}$.

We continue by considering a Lyapunov function;

$$\mathscr{L} = \mathbf{u}V^{-1}\mathbf{x}$$

Differentiating $\mathscr{L}$ along the solutions of (3.1), we have

$$\frac{d\mathscr{L}}{dt} = \mathbf{u}V^{-1}\frac{d\mathbf{x}}{dt} \leq \mathbf{u}V^{-1}(F-V)\mathbf{x} = \mathbf{u}(\mathscr{R}_0 - 1)\mathbf{x}$$

Case 1: If $\mathscr{R}_0 < 1$, the equality $\frac{d\mathscr{L}}{dt} = 0$ implies that $\mathbf{ux} = 0$ which lead to $E = I = V = 0$ by noting the positive components of $\mathbf{u}$. Hence, $\mathscr{R}_0 < 1$, equation (3.1) yields $S = S_0$, $M = M_0$ and $E = I = R = V = 0$. Thus, the invariant set on which $\frac{d\mathscr{L}}{dt} = 0$ contains only one point, DFE.
Case 2: If $\mathscr{R}_0 = 1$ then the equality $\frac{d\mathscr{L}}{dt} = 0$ implies that

$$\left(\frac{\beta_E(M)S}{S_0} + \frac{\alpha\beta_I(M)}{k} + \frac{(k\xi_1(M) + \alpha\xi_2(M))\beta_V(M)}{k\rho} - \frac{\alpha+\mu}{S_0}\right)E$$

$$+\left(\frac{S}{S_0}\beta_I(M) - \beta_I(\frac{\chi}{\nu})\right)I + \left(\frac{S}{S_0}\beta_V(M) - \beta_V(\frac{\chi}{\nu})\right)V = 0$$

One can easily see that

$$\frac{S}{S_0}\beta_I(M) - \beta_I(\frac{\chi}{\nu}) \leq 0, \quad \frac{S}{S_0}\beta_V(M) - \beta_V(\frac{\chi}{\nu}) \leq 0 \text{ and}$$

$$\begin{aligned}
&\frac{\beta_E(M)S}{S_0} + \frac{\alpha\beta_I(M)}{k} + \frac{(k\xi_1(M) + \alpha\xi_2(M))\beta_V(M)}{k\rho} - \frac{\alpha+\mu}{S_0} \\
&\leq \frac{\alpha+\mu}{S_0}\left(\frac{\beta_E(\frac{\chi}{\nu})S_0}{(\alpha+\mu)} + \frac{\alpha\beta_I(\frac{\chi}{\nu})S_0}{(\alpha+\mu)k} + \frac{(k\xi_1(\frac{\chi}{\nu}) + \alpha\xi_2(\frac{\chi}{\nu}))\beta_V(\frac{\chi}{\nu})S_0}{\rho(\alpha+\mu)k} - 1\right) \\
&= \frac{\alpha+\mu}{S_0}(\mathscr{R}_0 - 1) = 0
\end{aligned}$$

Note that $M_0 = \frac{\chi}{\nu}$

Thus, we have either $E = I = V = 0$, or $\beta_E(M) = \beta_E(\frac{\chi}{\nu})$, $\beta_I(M) = \beta_I(\frac{\chi}{\nu})$, $\beta_V(V) = \beta_V(\frac{\chi}{\nu})$, and $S = S_0$. As processed before, each of these cases would indicate the DFE X_0 is the only invariant set on $\left\{(S,E,I,R,V,M) \in \Omega : \frac{d\mathscr{L}}{dt} = 0\right\}$.

Therefore, in either case, the largest invariant set on which $\frac{d\mathscr{L}}{dt} = 0$ consists of the singleton $X_0 = (S_0, 0, 0, 0, 0, M_0)$. By LaSalle's invariant principle (LaSalle 1976), the DFE is globally asymptotically stable in Ω if $\mathscr{R}_0 \leq 1$.

In contrast, if $\mathscr{R}_0 > 1$, then it follows from the continuity of vector fields that $\frac{d\mathscr{L}}{dt} = 0$ in a neighborhood of the DFE in $\mathring{\Omega}$. Thus the DFE is unstable by the Lyapunov stability theory. The last part can be proved by the persistent theory[33] which is similar to the proof of Theorem 2.5 in Gao and Ruan (2011)[34].

We proceed to conduct an analysis on the global asymptotic stability of the endemic equilibrium. For simplicity, we denote;

$\beta_E(M) = \beta_E$, $\beta_I(M) = \beta_I$, $\beta_V(M) = \beta_V$, $\beta_E(M_*) = \beta_E^*$, $\beta_I(M_*) = \beta_I^*$, $\beta_V(M_*) = \beta_V^*$.

To establish the global stability of X_*, we assume

$$\left(1 - \frac{\beta_E E}{\beta_E^* E_*}\right)\left(1 - \frac{M\beta_E^* E_*}{M_*\beta_E E}\right) \geq 0 \tag{4.5}$$

for $0 \leq E \leq \frac{\Lambda}{\mu}$ and $M_0 \leq M \leq M_{\max}$.

Theorem 4.0.2. *Suppose that equation (4.5) holds; $\xi_1(M) \equiv \xi_1$ and $\xi_2(M) \equiv \xi_2$ are constants; $\sigma = 0$, and $\beta_E(M)E$, $\beta_I(M)I$ and $\beta_V(M)V$ are non-decreasing functions of the variable M. If $\mathscr{R}_0 > 1$, then the unique endemic equilibrium X_* of (1) is globally asymptotically stable in $\mathring{\Omega}$.*

Proof

Let $L_Z = \int_{Z_*}^{Z} \frac{X - Z_*}{X} dX$ for $Z > 0$ where $Z_* > 0$ and Z can be replaced by S, E, I, V or M. Clearly $L_Z \leq 0$ with the equality holding if and only if $Z = Z_*$. Differentiating L_S, L_E, L_I, L_V and L_M along the solutions of (3.1) with the equlibrium equations in (4.1) yields;

$$\begin{aligned}
L_S' &= \left(1 - \frac{S_*}{S}\right) S' = \left(1 - \frac{S_*}{S}\right)\left[\beta_E^* S_* E - \beta_E SE + \beta_I^* S_* I - \beta_I SI + \beta_V^* S_* V - \mu S\left(1 - \frac{S_*}{S}\right)\right] \\
&\leq \left(1 - \frac{S_*}{S}\right)\left[\beta_E^* S_* E - \beta_E SE + \beta_I^* S_* I - \beta_I SI + \beta_V^* S_* V\right] \\
&= \beta_E^* E_* S_*\left(1 - \frac{S_*}{S} - \frac{\beta_E ES}{\beta_E^* E_* S_*} + \frac{\beta_E E}{\beta_E^* E_*}\right) + \beta_I^* I_* S_*\left(1 - \frac{S_*}{S} - \frac{\beta_I IS}{\beta_I^* I_* S_*} + \frac{\beta_I I}{\beta_I^* I_*}\right) \\
&+ \beta_V^* V_* S_*\left(1 - \frac{S_*}{S} - \frac{\beta_V VS}{\beta_V^* V_* S_*} + \frac{\beta_V V}{\beta_V^* V_*}\right)
\end{aligned}$$

$$
\begin{aligned}
L'_E &= \left(1-\frac{E_*}{E}\right)E' = \left(1-\frac{E_*}{E}\right)\left[\beta_E SE+\beta_I SI+\beta_V SV-(\alpha+\mu)E\right] \\
&= \beta_E^* E_* S_* \left(1-\frac{E}{E_*}+\frac{\beta_E ES}{\beta_E^* E_* S_*}-\frac{\beta_E S}{\beta_E^* S_*}\right)+\beta_I^* I_* S_* \left(1-\frac{E}{E_*}+\frac{\beta_I IS}{\beta_I^* I_* S_*}-\frac{\beta_I ISE_*}{\beta_I^* I_* S_* E}\right) \\
&+\beta_V^* V_* S_* \left(1-\frac{E}{E_*}+\frac{\beta_V VS}{\beta_V^* V_* S_*}-\frac{\beta_V VSE_*}{\beta_V^* V_* S_* E}\right)
\end{aligned}
$$

Adding L'_S and L'_E, we obtain the following the results,

$$
\begin{aligned}
L'_S+L'_E \leq{}& \beta_E^* E_* S_* \left(2-\frac{S_*}{S}-\frac{E}{E_*}+\frac{\beta_E E}{\beta_E^* E_*}-\frac{\beta_E S}{\beta_E^* S_*}\right)+\beta_I^* I_* S_* \left(2-\frac{S_*}{S}-\frac{E}{E_*}+\frac{\beta_I I}{\beta_I^* I_*}-\frac{\beta_I ISE_*}{\beta_I^* I_* S_* E}\right) \\
&+\beta_V^* V_* S_* \left(2-\frac{S_*}{S}-\frac{E}{E_*}+\frac{\beta_V V}{\beta_V^* V_*}-\frac{\beta_V VSE_*}{\beta_V^* V_* S_* E}\right)
\end{aligned}
$$

Notice that $x-1 \geq In(x)$ for $x>0$ and equality holds if and only if $x=1$. Together with (4.5) we find that;

$$
\begin{aligned}
&2-\frac{S_*}{S}-\frac{E}{E_*}+\frac{\beta_E E}{\beta_E^* E_*}-\frac{\beta_E S}{\beta_E^* S_*} \\
&=-\left(1-\frac{\beta_E E}{\beta_E^* E_*}\right)\left(1-\frac{M\beta_E^* E_*}{M_*\beta_E E}\right)+3-\frac{S_*}{S}-\frac{\beta_E S}{\beta_E^* S_*}-\frac{M\beta_E^* E_*}{M_*\beta_E E}-\frac{E}{E_*}+\frac{M}{M_*} \\
&\leq -\left(\frac{S_*}{S}-1\right)-\left(\frac{\beta_E S}{\beta_E^* S_*}-1\right)-\left(\frac{M\beta_E^* E_*}{M_*\beta_E E}-1\right)-\frac{E}{E_*}+\frac{M}{M_*} \\
&=\ln\left(\frac{S_*}{S}\frac{\beta_E S}{\beta_E^* S_*}\frac{M\beta_E^* E_*}{M_*\beta_E E}\right)-\frac{E}{E_*}+\frac{M}{M_*} \\
&=\frac{M}{M_*}-\ln\frac{M}{M_*}-\frac{E}{E_*}+\ln\frac{E}{E_*}
\end{aligned}
$$

Thus,

$$
\begin{aligned}
L'_S+L'_E \leq{}& \beta_E^* E_* S_* \left(\frac{M}{M_*}-\ln\frac{M}{M_*}-\frac{E}{E_*}+\ln\frac{E}{E_*}\right) \\
&+\beta_I^* I_* S_* \left[\left(\frac{\beta_I I}{\beta_I^* I_*}-1\right)\left(1-\frac{\beta_I^*}{\beta_I}\right)+\frac{I}{I_*}-\frac{E}{E_*}-\ln\frac{I}{I_*}+\ln\frac{E}{E_*}\right] \\
&+\beta_V^* V_* S_* \left[\left(\frac{\beta_V V}{\beta_V^* V_*}-1\right)\left(1-\frac{\beta_V^*}{\beta_V}\right)+\frac{V}{V_*}-\frac{E}{E_*}-\ln\frac{V}{V_*}+\ln\frac{E}{E_*}\right] \\
\leq{}&\beta_E^* E_* S_* \left(\frac{M}{M_*}-\ln\frac{M}{M_*}-\frac{E}{E_*}+\ln\frac{E}{E_*}\right)+\beta_I^* I_* S_* \left(\frac{I}{I_*}-\frac{E}{E_*}-\ln\frac{I}{I_*}+\ln\frac{E}{E_*}\right) \\
&+\beta_V^* V_* S_* \left(\frac{V}{V_*}-\frac{E}{E_*}-\ln\frac{V}{V_*}+\ln\frac{E}{E_*}\right)
\end{aligned}
$$

The last inequality follows assumption (2) and Theorem 4.0.2 which implies that $\beta_D(M)$ and $\beta_D(M)D$, where D represents E, I or$V$ are non-increasing and non-decreasing respectively. Therefore

$$1-\frac{\beta_D^*}{\beta_D}\leq 0 \Longleftrightarrow D* \leq D \Longleftrightarrow \frac{\beta_D D}{\beta_D^* D_*}-1\geq 0$$

Similarly, we obtain the following;

$$L_I'=\left(1-\frac{I_*}{I}\right)I'=\alpha E_*\left(\frac{E}{E_*}-\frac{I}{I_*}-\frac{I_*E}{IE_*}+1\right)\leq \alpha E_*\left(\frac{E}{E_*}-\frac{I}{I_*}+\ln\frac{I}{I_*}-\ln\frac{E}{E_*}\right)$$

$$\begin{aligned}L_V'&=\left(1-\frac{V_*}{V}\right)V'=\xi_1 E_*\left(\frac{E}{E_*}-\frac{V}{V_*}-\frac{V_*E}{VE_*}+1\right)+\xi_2 I_*\left(\frac{I}{I_*}-\frac{V}{V_*}-\frac{V_*I}{VI_*}+1\right)\\&\leq \xi_1 E_*\left(\frac{E}{E_*}-\frac{V}{V_*}+\ln\frac{V}{V_*}-\ln\frac{E}{E_*}\right)+\xi_2 I_*\left(\frac{I}{I_*}-\frac{V}{V_*}+\ln\frac{V}{V_*}-\ln\frac{I}{I_*}\right)\end{aligned}$$

$$\begin{aligned}L_M'&=\left(1-\frac{M_*}{M}\right)M'=-\chi\frac{M}{M_*}\left(1-\frac{M_*}{M}\right)^2+\eta I_*\left(\frac{I}{I_*}-\frac{M}{M_*}-\frac{M_*I}{MI_*}+1\right)\\&\leq \eta I_*\left(\frac{I}{I_*}-\frac{M}{M_*}+\ln\frac{M}{M_*}-\ln\frac{I}{I_*}\right)\end{aligned}$$

We proceed to consider the Lyapunov function below.

$$\mathscr{L}=L_S+L_E+c_1L_I+c_2L_V+c_3L_M$$

where $c_i>0$, for $(i=1,2,3)$ are constants to be determined. It is easy to verify that $\mathscr{L}\geq 0$ for all $S,E,I,V,M>0$ and,

$$\begin{aligned}\mathscr{L}'\leq&(\beta_E^*E_*S_*+\beta_I^*I_*S_*+\beta_V^*V_*S_*-c_1\alpha E_*-c_2\xi_1E_*)\left(\ln\frac{E}{E_*}-\frac{E}{E_*}\right)\\&+(\beta_I^*I_*S_*-c_1\alpha E_*+c_2\xi_2I_*+c_3\eta I_*)\left(\frac{I}{I_*}-\ln\frac{I}{I_*}\right)\\&+(\beta_V^*V_*S_*-c_2(\xi_1E_*+\xi_2I_*))\left(\frac{V}{V_*}-\ln\frac{V}{V_*}\right)\\&+(\beta_E^*E_*S_*-c_3\eta I_*)\left(\frac{M}{M_*}-\ln\frac{M}{M_*}\right)\\=&0\end{aligned}$$

Taking $c_1 = \frac{\beta_I^* I_* S_*}{\alpha E_*} + \frac{\beta_E^* E_* S_*}{\alpha E_*} + \frac{\xi_2 \beta_V^* V_* S_*}{(k\xi_1 + \alpha\xi_2) E_*}$, $c_2 = \frac{k\beta_V^* V_* S_*}{(k\xi_1 + \alpha\xi_2) E_*}$ and $c_3 = \frac{\beta_E^* E_* S_*}{\eta I_*}$

It is observed by direct calculation that the right-hand side of the inequality is zero, with the equality holding if and only if $(S,E,I,V,M) = (S_*,E_*,I_*,V_*,M_*)$ This shows that $\mathscr{L}' \leq 0$ with the chosen positive constants c_1, c_2, and c_3. Moreover, if $\mathscr{L}' = 0$, then there exists a constant $\hat{q}$ such that

$$S = S_*, \quad E = \hat{q}E, \quad I = \hat{q}I_*, \quad V = \hat{q}V_*, \quad M = \hat{q}M_* \tag{4.6}$$

However, by the last equation of (4.1),$0 = \chi + \eta\hat{q}I_* - \nu\hat{q}M_*$ This implies that $\hat{q} = 1$. Meanwhile, $R = R_*$ which follows from the third equation of (4.1). Thus, the largest invariant set for which $\mathscr{L}' = 0$ contains only the EE, that is X_*. Therefore, by LaSalle's invariant principle [35], the EE is globally asymptotically stable in $\mathring{\Omega}$ when $\mathscr{R}_0 > 1$.

CHAPTER 5

NUMERICAL SIMULATIONS AND RESULTS

We now run simulations on the proposed model to obtain visual interpretations of the disease transmission at the disease-free equilibrium and the endemic equilibrium. We also run data fitting simulations with reported data from Wuhan, the epicenter of the coronavirus disease and the state of Tennessee [36, 7]. In exploring the disease dynamics at selected values of $\mathscr{R}_0 = 2.672$ and $\mathscr{R}_0 = 0.663$, we used most parameter estimates from Yang and Wang (2020) [31]. We expressed the transmission and shedding rates functions as;

$$\begin{aligned} &\beta_E = \beta_{E0} - bM \quad \beta_I = \beta_{I0} - bM \quad \beta_V = \beta_{V0} - bM \\ &\xi_1 = \xi_{1_0} - cM \qquad \xi_2 = \xi_{2_0} - cM \end{aligned} \tag{5.1}$$

where β_{E0}, β_{I0}, β_{V0}, b and c are all positive valued constants. We initially make calculated assumptions on the values of χ, η, ν and c as their estimates are not available in published models and eventually estimate their actual values in our data fitting using the standard least squares method. In the table below we define and indicate the parameters and their estimated values used in our model simulations. The initial condition was set as $(S(0), E(0), I(0), R(0), M(0)) = (8998505, 1000, 475, 10, 10000, 5)$

Table 5.1
Definitions and Estimates of Model Parameters

Parameter	Definition	Est. Mean $\mathscr{R}_0 > 1$	Est. Mean $\mathscr{R}_0 < 1$
Λ	Population influx rate	271.23/d	271.23/d
μ	Natural death rate	3.01×10^{-5}/d	3.01×10^{-5}/d
β_{E0}	Transmission rate const. between S and E	3.11×10^{-8}/p/d	0.8×10^{-8}/p/d
β_{I0}	Transmission rate const. between S and I	0.62×10^{-8}/p/d	0.15×10^{-8}/p/d
β_{V0}	Transmission rate const. between S and V	1.02×10^{-8}/p/d	$.2 \times 10^{-8}$/p/d
b	Transmission adjustment coefficient	0.02×10^{-9}/p/d	0.02×10^{-9}/p/d
c	Shedding adjustment coefficient	0.5×10^{-9}ml/d	0.5×10^{-9}ml/d
ξ_{1_0}	Shedding rate constant from E	5.0×10^{-8}ml/d	1.7×10^{-8}ml/d
ξ_{2_0}	Shedding rate constant from I	4.0×10^{-8}ml/d	1.5×10^{-8}ml/d
α^{-1}	Incubation period	7d	7d
ρ	Virus removal rate	1/d	1d
ω	Disease-induced death rate	0.01/d	0.01/d
γ	Recovery rate	1/15per d	1/15per d
σ	Waning rate of immunity	0.4/d	0.4/d
χ	Awarneness programs influx	2.5d	2.5d
η	Disease prevalence rate	0.2×10^{-8}/d	0.2×10^{-8}/d
ν	Decay rate of awareness programs	0.5/d	0.5/d

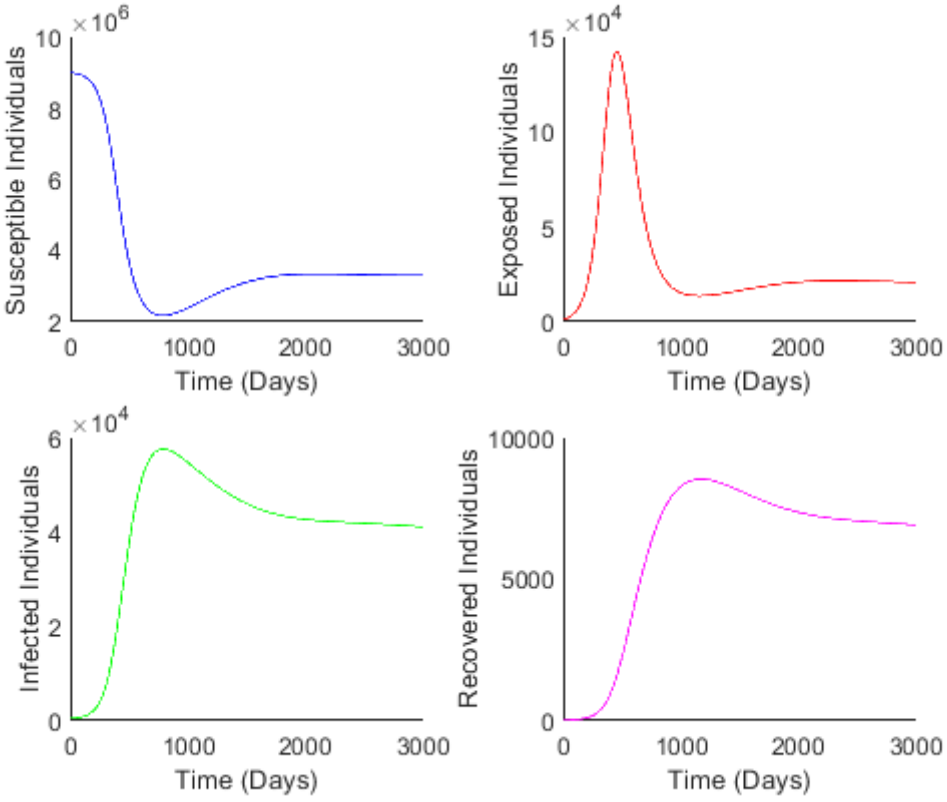

Figure 5.1
Model simulations showing the compartmental flow at $\mathscr{R}_0 = 2.672$

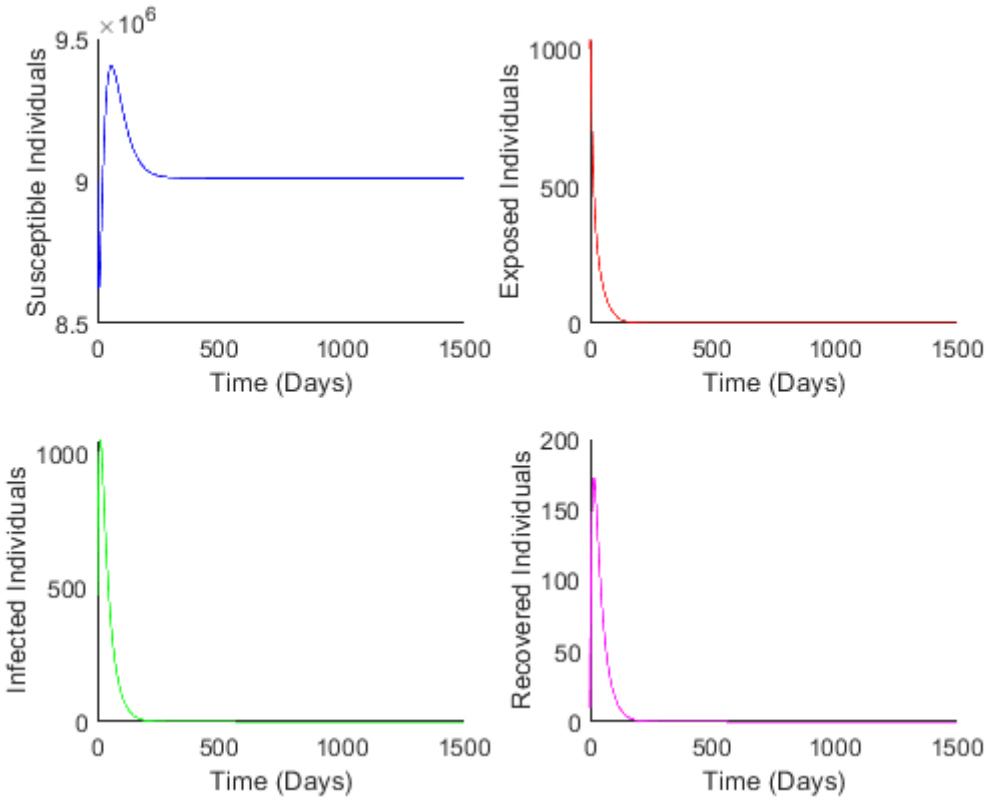

Figure 5.2
Model simulations showing the compartmental flow at $\mathscr{R}_0 = 0.663$

To demonstrate the global stability of the DFE and EE we proceed with the plotted phase portraits using the initial conditions below;

Initial condition1 (magenta)= (8998505 1000 475 10 100000 5)

Initial condition2 (green)=(8992500 5000 2475 15 110000 50)

Initial condition3 (blue)=(8978990 20000 9000 100 150000 25)

Initial condition4 (black)=(8949340 35000 23250 500 20000 1000)

Initial condition5 (red)=(8932090 50000 25000 1000 30000 100)

Initial condition6 (yellow)=(8937090 45000 24000 2000 25000 500)

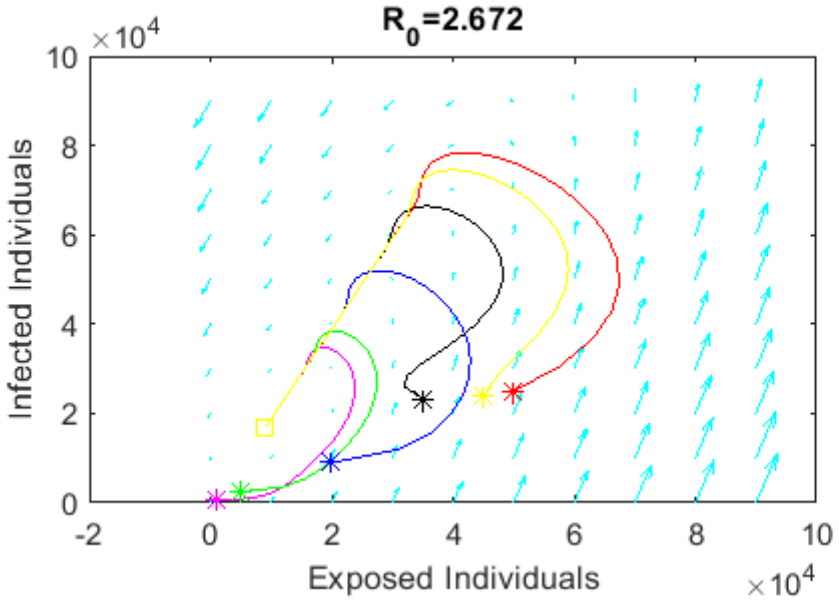

Figure 5.3
A phase portrait in the Exposed-Infected plane at $\mathscr{R}_0 = 2.672$

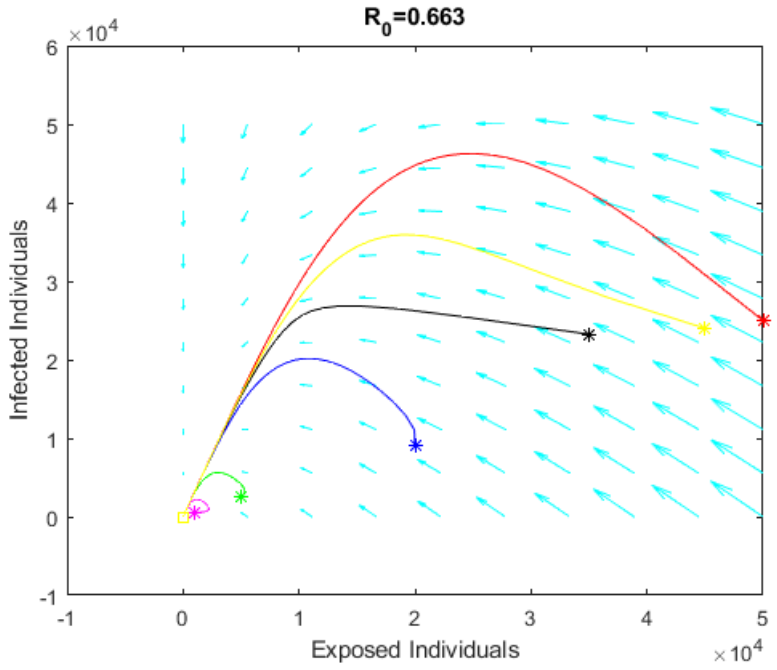

Figure 5.4
A phase portrait in the Exposed-Infected plane at $\mathscr{R}_0 = 0.663$

The table 5.2 was set up based on the daily reported infection data from Wuhuan (January 23 to February 10). We fit our model to the data by using the standard least squares method. Based on reported data, the initial condition is set as $(S(0), E(0), I(0), R(0), V(0), M(0)) = (8998505, 1000, 475, 10, 10000, M(0))$[36]

Table 5.2
Estimates of Model Parameters

Parameter	Estimated Mean	Source
Λ	271.23/day	[31, 37]
μ	3.01×10^{-5}/day	[31, 37]
β_{E0}	3.11×10^{-8}/person/day	[31, 38]
β_{I0}	0.62×10^{-8}/person/day	[31, 38]
β_{V0}	1.03×10^{-8}/person/day	[31]
b	fitting by data	-
c	fitting by data	-
ξ_{1_0}	2.30/person/ml/day	[31]
ξ_2	0ml/day	-
α^{-1}	7days	[31, 39]
ρ	1 per day	[31, 40]
ω	0.01per day	[31, 37]
γ	$1/15$per day	[31, 39]
σ	0per day	-
χ	0 per day	-
η	fitting by data	-
ν	fitting by data	-

Based on the parameter values from data fitting, we are able to evaluate the basic reproduction number $\mathscr{R}_0 = 2.899$. Specifically, we find that

$$\mathscr{R}_{0E} = 1.959; \quad \mathscr{R}_{0I} = 0.727; \quad \mathscr{R}_{0V} = 0.213;$$

The normalized mean square error (NMSE) for the data fitting is found as 0.05372.

Parameter estimates from data fitting from setting $M(0) = 0$

Table 5.3
Estimates from Data Fitting

Parameter	Fitting value	95% Confidence Interval
b	20.539×10^{-9}/person/day	$(0, 0.0016)$
c	4.0239×10^{-12}ml/day	$(0, 2.436)$
η	2.762×10^{-11}/day	$(0, 0.00219)$
ν	2.253×10^{-11}/day	$(0, 0.0455)$

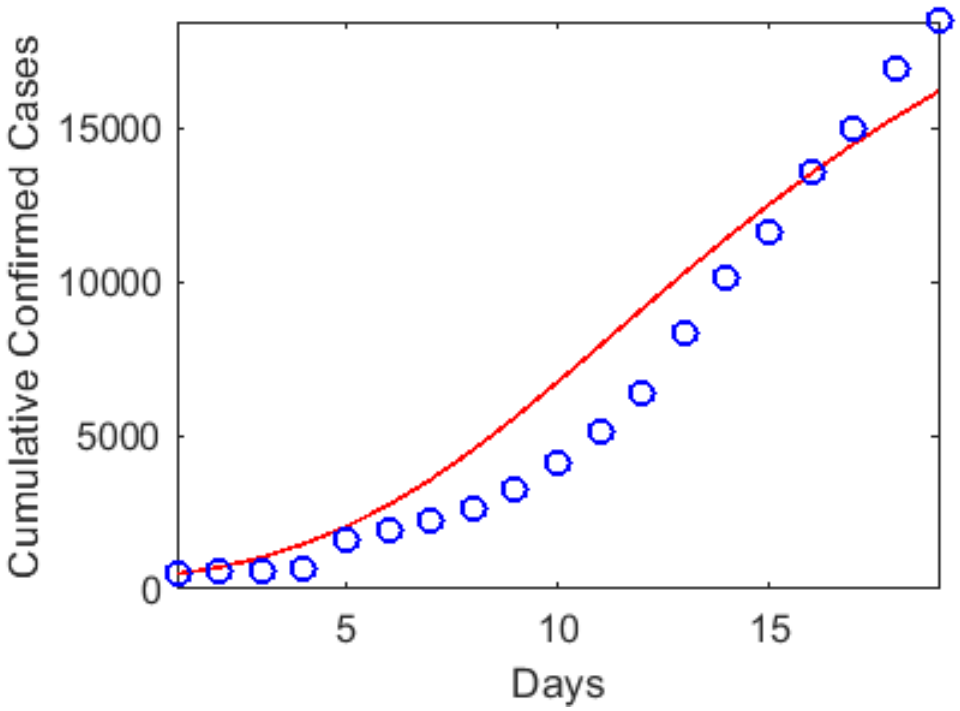

Figure 5.5
Simulation result of cumulative confirmed cases in Wuhan

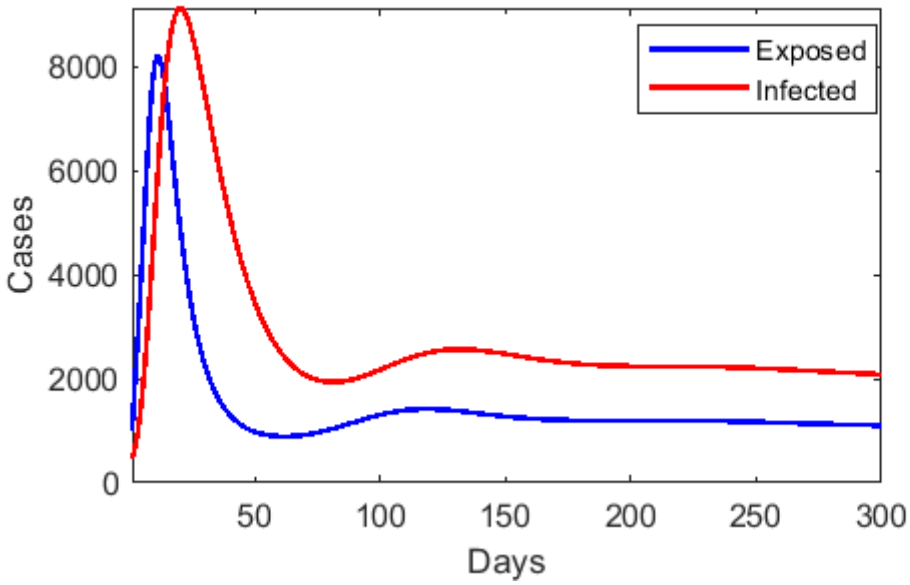

Figure 5.6
Plot showing the evolution of exposed and infected cases at $\mathscr{R}_0 = 2.899$

Table 5.4
Estimates of Parameters from Data Fitting

Parameter	Fitting value	95% Confidence Interval
b	8.0389×10^{-12}/person/day	$(0, 19.281\times10^{-9})$
c	2.30×10^{-10}ml/day	$(0, 0.586)$
η	0.0009/day	$(0, 0.113)$
ν	1.1×10^{-7}/day	$(0, 9.33)$

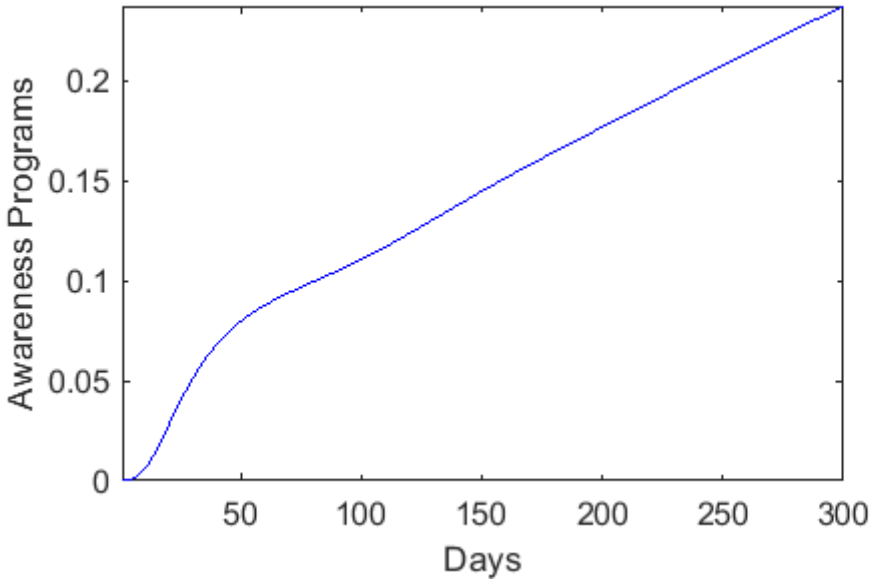

Figure 5.7
A growth curve of awareness programs in Wuhan at $M(0) = 0$

Below are the data fitting results obtained by extending the initial reported data (January 23, 2020 to March 1, 2020);

The values for the basic reproduction unit in all three transmission routes remained same [36].

The normalized mean square error (NMSE) for the data fitting is found as 0.0389.

Parameter estimates from data fitting from setting $M(0) = 5$

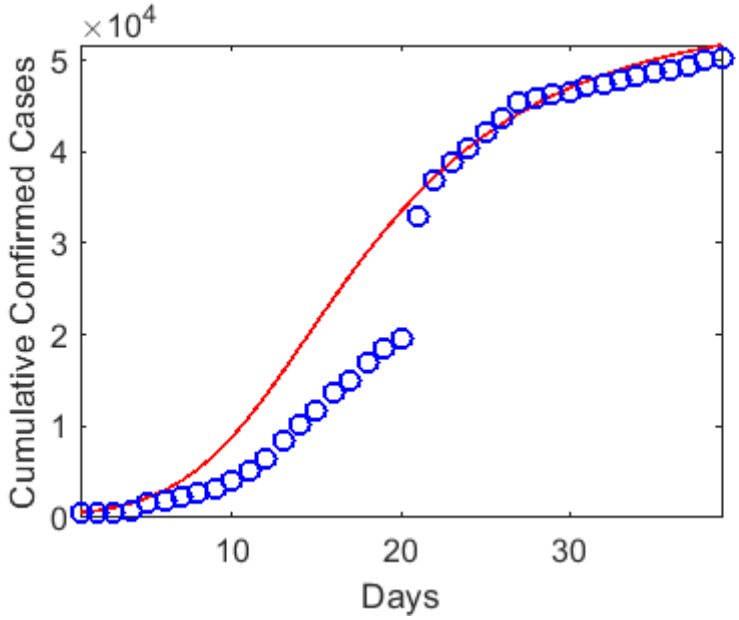

Figure 5.8
The cumulative confirmed cases from Jan 23, 2020-Mar 1, 2020 in Wuhan

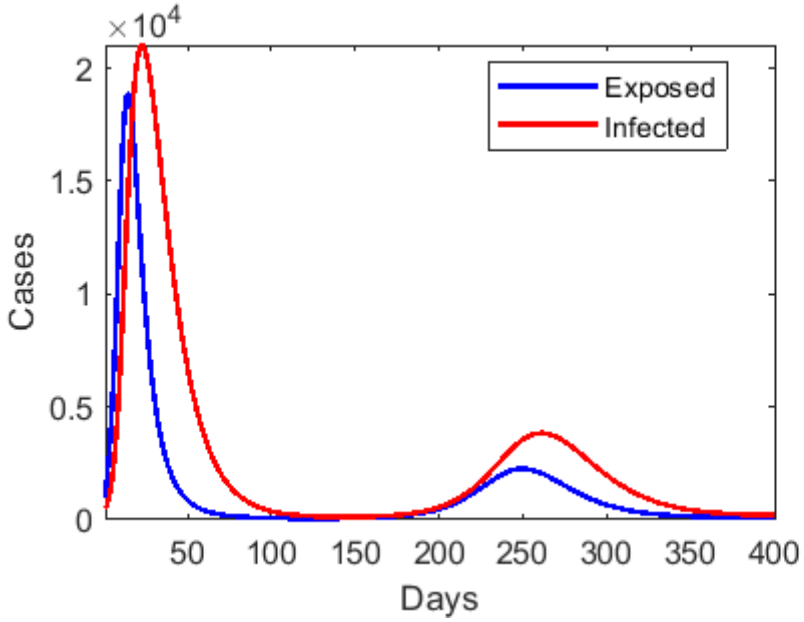

Figure 5.9
A plot showing the estimated growth of exposed and infected cases in Wuhan

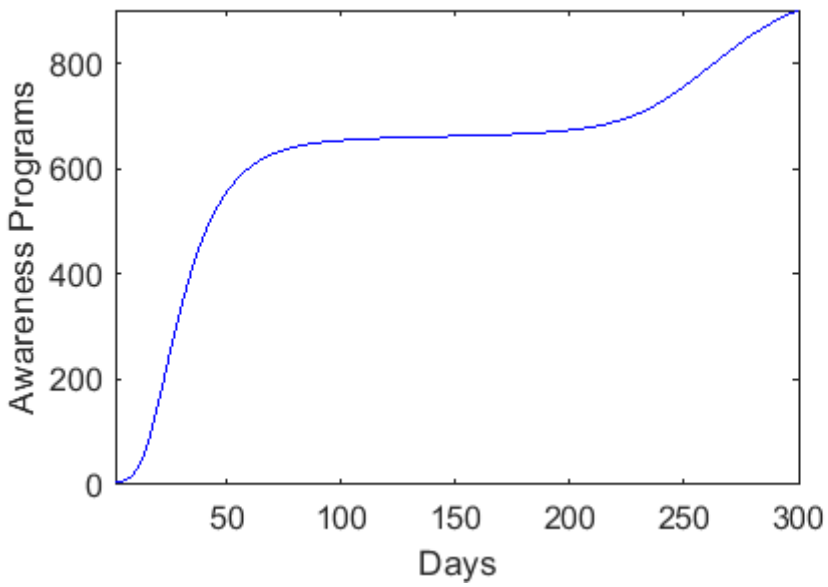

Figure 5.10
Growth curve of awareness programs in Wuhan in 300 days

We now consider reported data from the state of Tennessee in the USA particularly, the daily reported data from May 1, 2020 to July 14, 2020[7]. Due to the change in geographical setting we adjust the major affected parameters and initial conditions whiles maintaining transmission coeffiecient estimates from Wuhan [31, 38]. We fit our model to the data by using the standard least squares method to obtain values for the awareness programs growth in the state. Based on the reported data, the initial condition was set as $(S(0),E(0),I(0),R(0),V(0),M(0)) = (6896375,2000,1100,15,10000,0)$. Based on the results from the data fitting, we evaluated the basic reproduction number at; $\mathscr{R}_0 = 2.223$. Specifically, we found;

$$\mathscr{R}_{0E} = 1.502; \quad \mathscr{R}_{0I} = 0.558; \quad \mathscr{R}_{0V} = 0.1634;$$

The normalized mean square error (NMSE) for the data fitting is found as 0.05711.

Table 5.5
Estimates of Model Parameters

Parameter	Estimated Mean	Source
Λ	198.49/day	[41]
μ	2.88×10^{-5}/day	[42]
β_{E0}	3.11×10^{-8}/person/day	[31, 38]
β_{I0}	0.62×10^{-8}/person/day	[31, 38]
β_{V0}	1.03×10^{-8}/person/day	[31, 38]
b	fitting by data	-
c	fitting by data	-
ξ_{1_0}	2.30/person/ml/day	[31]
ξ_2	0ml/day	-
α^{-1}	7days	[31, 39]
ρ	1 per day	[31, 40]
ω	0.01per day	[31, 37]
γ	$1/15$per day	[31, 39]
σ	0per day	-
χ	0 per day	-
η	fitting by data	-
ν	fitting by data	-

Table 5.6
Estimates of Parameters from Data Fitting

Parameter	Fitting value	95% Confidence Interval
b	8.039×10^{-10}/person/day	$(0, 2.703)$
c	8.30×10^{-10}ml/day	$(0, 0.241)$
η	0.005/day	$(0, 4.114)$
ν	0.0001/day	$(0, 7.586 \times 10^{-9})$

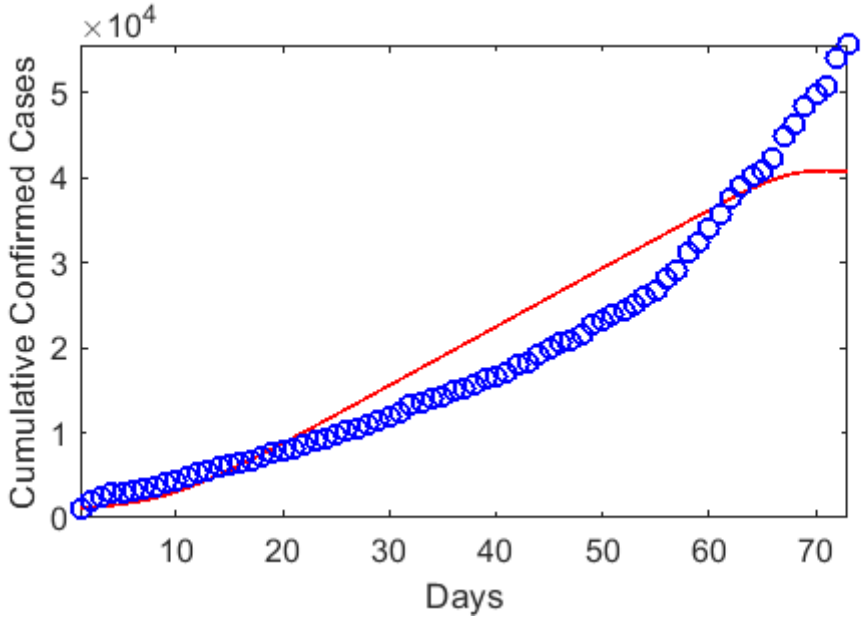

Figure 5.11
Cumulative confirmed cases in Tennessee with Wuhan transmission coefficient

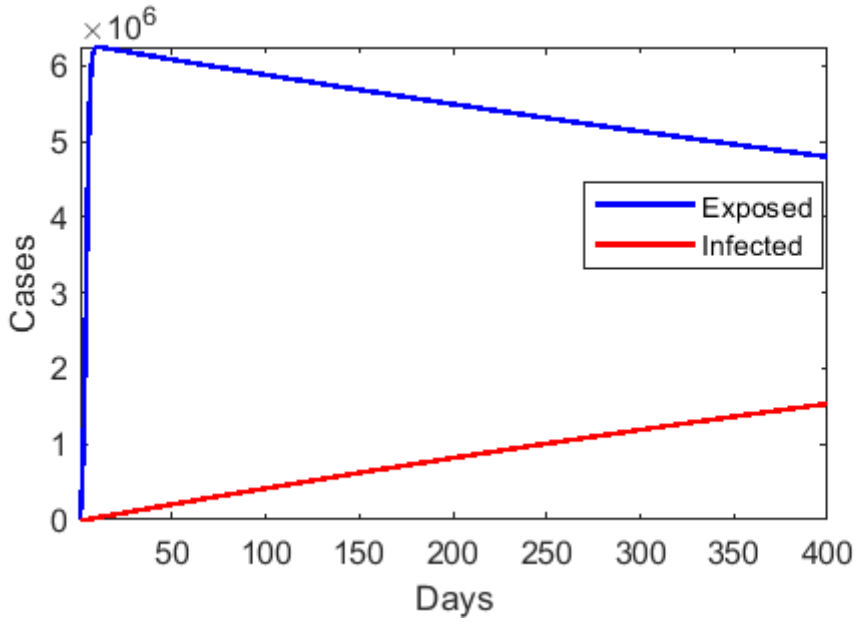

Figure 5.12
A data fitting result showing growth of exposed and infected cases for 400 days

Table 5.7
Estimates of Model Parameters

Parameter	Estimated Mean	Source
Λ	198.49/day	[41]
μ	2.88×10^{-5}/day	[42]
β_{E0}	fitting by data	
β_{I0}	fitting by data	
β_{V0}	fitting by data	
b	8.0389×10^{-12}/person/day	Table5.6
c	2.30×10^{-10}ml/day	Table5.6
ξ_{1_0}	2.30person/ml/day	[31]
ξ_{2_0}	0ml/day	-
α^{-1}	7days	[31, 39]
ρ	1 per day	[31, 40]
ω	0.01per day	[31, 37]
γ	$1/15$per day	[31, 39]
σ	0per day	-
χ	0 per day	-
η	0.0009/day	Table5.6
ν	1.1×10^{-7}/day	Table5.6

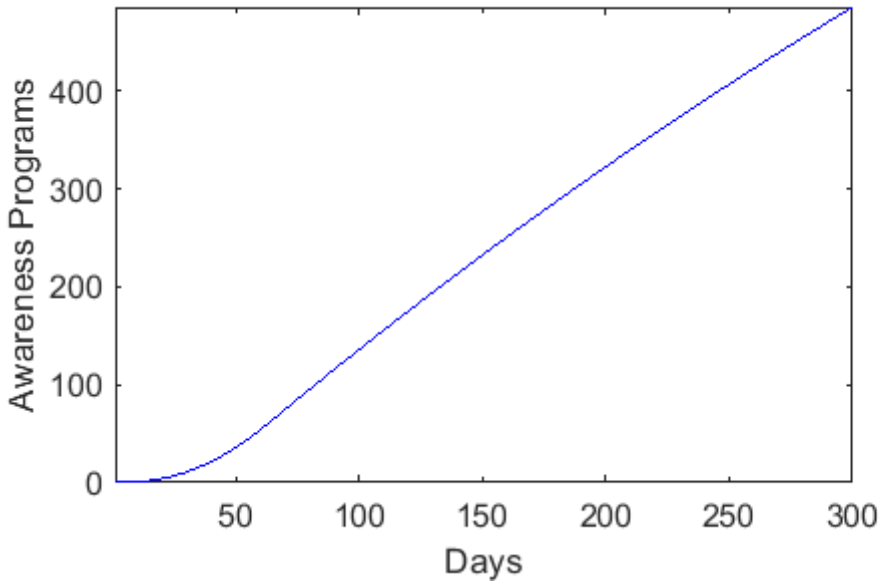

Figure 5.13
Growth of awareness programs in Tennessee for 300 days

The results derived from the data fitting above showed some abnormalities evident in Figure 5.12.Thus we change the parameters to be fitted to find the transmission rate coefficients as indicated in the table below. The results obtained were as follows, the basic reproduction

Table 5.8
Estimates of Parameters from Data Fitting

Parameter	Fitting value	95% Confidence Interval
β_{E0}	11.457×10^{-9}/person/day	$(10.384\times10^{-9}, 12.531\times10^{-9})$
β_{I0}	3.660×10^{-9}/person/day	$(3.010\times10^{-9}, 4.310\times10^{-9})$
β_{V0}	6.523×10^{-9}/person/day	$(6.320\times10^{-9}, 6.727\times10^{-9})$

number was evaluated at; $\mathscr{R}_0 = 0.8621$. Specifically,

$$\mathscr{R}_{0E} = 0.5145; \quad \mathscr{R}_{0I} = 0.2569; \quad \mathscr{R}_{0V} = 0.0907;$$

The normalized mean square error (NMSE) for the data fitting is found as 0.04391.

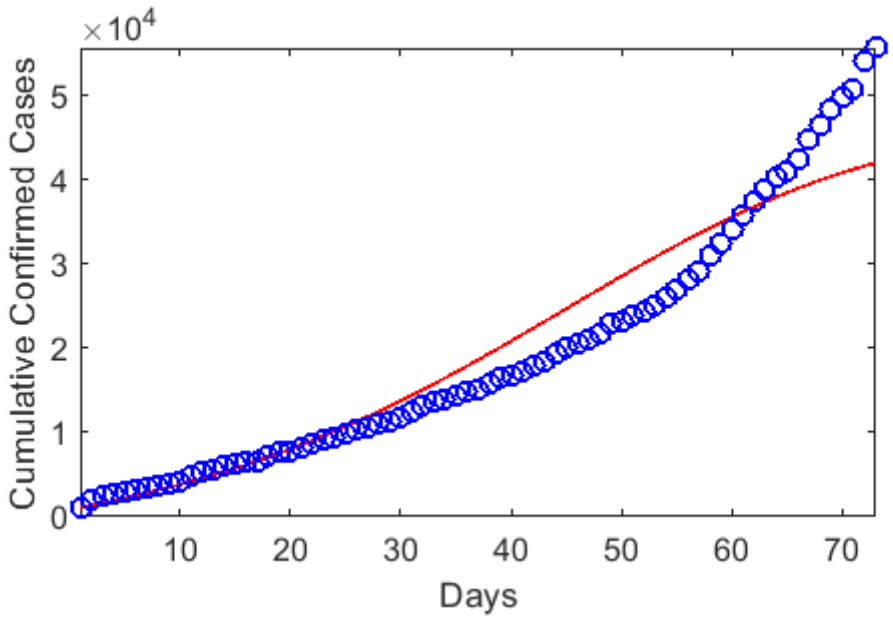

Figure 5.14
Cumulative confirmed cases from May 1, 2020-July 14,2020 in Tennessee

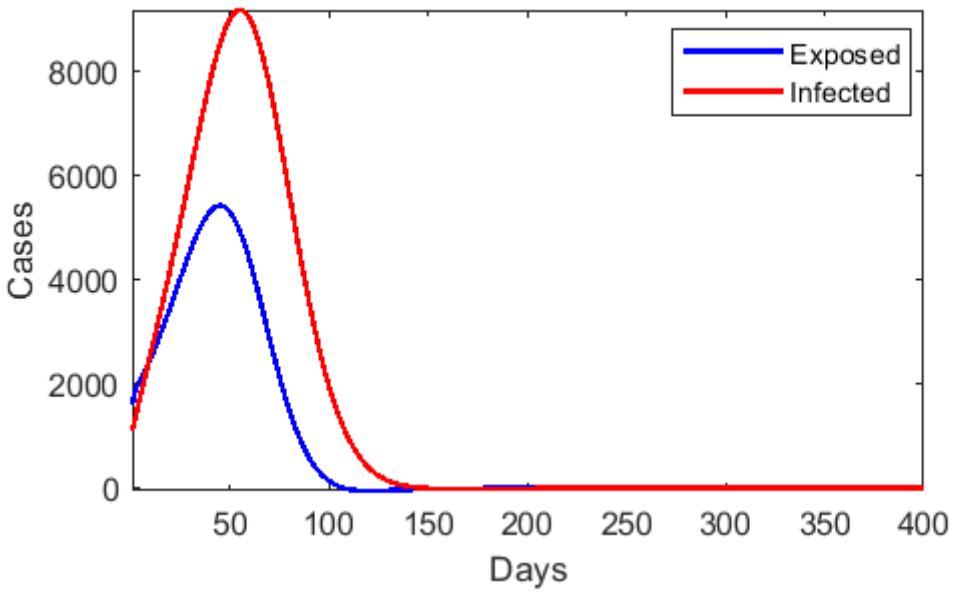

Figure 5.15
Growth curve of exposed and infected cases for 400 days

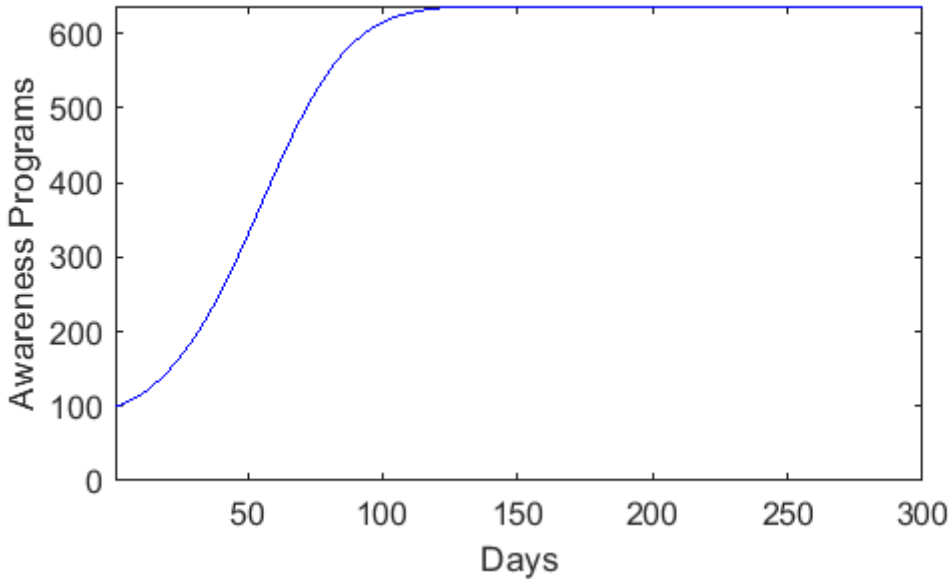

Figure 5.16
Estimated growth curve based on reported data from Tennessee

We also fit our model to the reported data from November 1st- December 16th 2020 by using the standard least squares method [7]. The initial condition was set as $(S(0), E(0), I(0), R(0), V(0), M(0))$ $(6896375, 2000, 800, 10, 10000, 500)$. Below are the results obtained. $\mathscr{R}_0 = 1.886$.

Table 5.9
Estimates of Parameters from Data Fitting

Parameter	Fitting value	95% Confidence Interval
β_{E0}	2.7979×10^{-8}/person/day	$(0, 7.445\times10^{-7})$
β_{I0}	5.4×10^{-9}/person/day	$(0, 5.022\times10^{-4})$
β_{V0}	1.0613×10^{-8}/person/day	$(0, 1.421\times10^{-7})$

Specifically, we find that

$$\mathscr{R}_{0E} = 1.357; \quad \mathscr{R}_{0I} = 0.324; \quad \mathscr{R}_{0V} = 0.205;$$

The normalized mean square error (NMSE) for the data fitting is found as 0.00636.

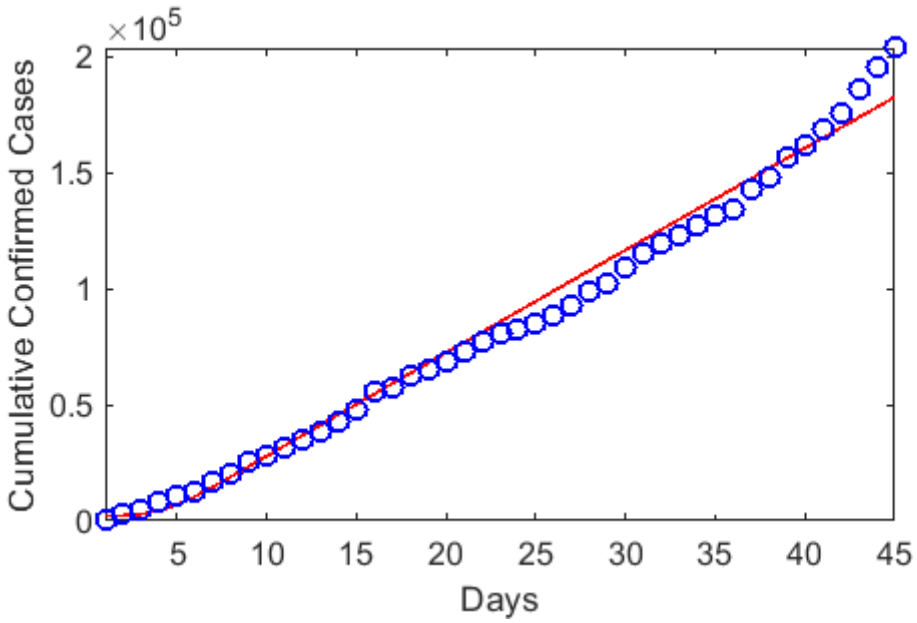

Figure 5.17
Cumulative confirmed cases from Nov. 1, 2020-Dec.15, 2020 in Tennessee

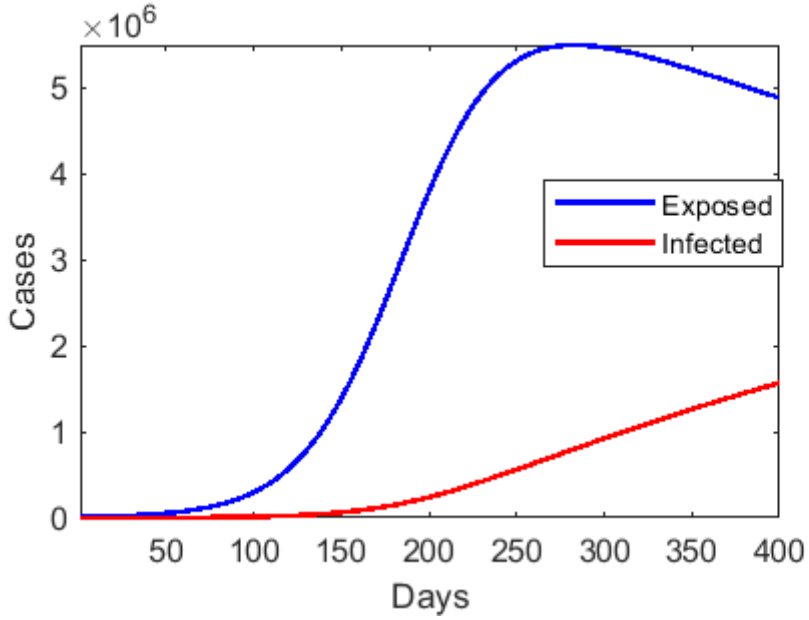

Figure 5.18
A data fitting result of growth curve of exposed and infected cases in Tennessee

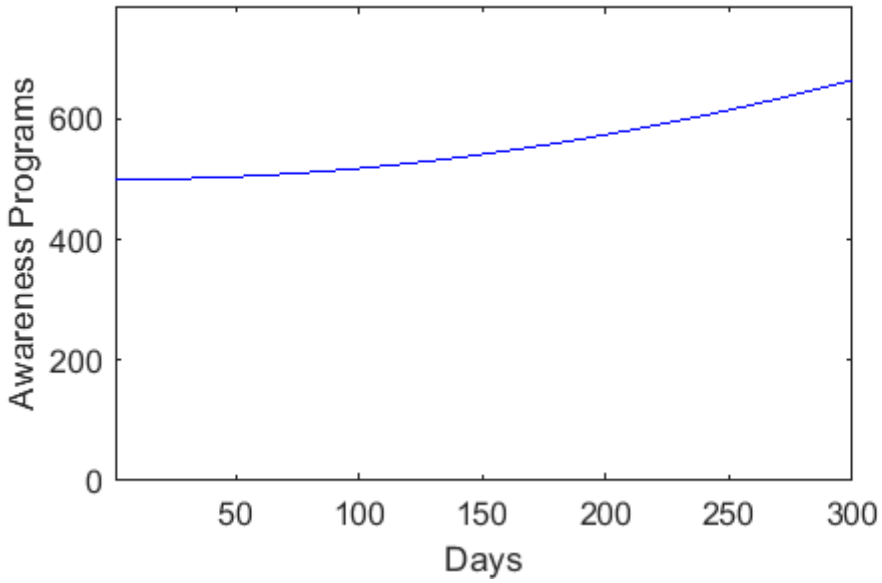

Figure 5.19
A growth curve of awareness programs in Tennessee at $M(0) = 500$

CHAPTER 6

CONCLUSION

In this study, we examined the extent of impact of intervention programs on the spread of the coronavirus disease 2019 by developing and discussing a modified SEIR model. Specifically, the model was expanded to consider the virus concentration in the environment and the growth dynamics of awareness programs created to mitigate the spread. The transmission rate functions of the model were expressed as decreasing functions of the awareness programs, M. We conducted a thorough analysis of the model and applied it in our study of reported data from Wuhan, China and the state of Tennessee in the USA. In order to facilitate the assessment of the intervention programs on the virus dissemination via all transmission routes, we itemized the basic reproduction threshold parameter, $\mathscr{R}_0$ into $\mathscr{R}_{0E}$, $\mathscr{R}_{0I}$ and $\mathscr{R}_{0V}$. The $\mathscr{R}_{0E}$ represented the infection via direct transmission route from exposed individuals. $\mathscr{R}_{0I}$ measured infection via direct transmission route from infected individuals and $\mathscr{R}_{0V}$, the indirect transmission from the virus concentration in the environment.

Our equilibrium analysis demonstrated that the dynamics of the disease shows a regular threshold when $\mathscr{R}_0 = 1$. We also proved that when $\mathscr{R}_0 < 1$ the disease-free equilibrium X_0 is globally asymptotically stable and at $\mathscr{R}_0 > 1$ the endemic equilibrium X_* is globally asymptotically stable (Figures 5.1, 5.2, 5.3, 5.4). Results from our numerical simulations show a transition of the disease occurrence from the endemic state to a disease-free state as the number of control measures increases. In particular, our data fitting result of Wuhan (reported data from January 23, 2020- February 10, 2020[36]) estimated $\mathscr{R}_0 = 2.899$ which is less than earlier recorded estimates of $\mathscr{R}_0$[31, 38]. Our simulations also highlighted the possibility of reaching a disease free equilibrium in the data fitting results of Tennessee (Figures 5.15, 5.16). $\mathscr{R}_0$ was estimated at 0.8621 with the initial awareness program set at $M(0) = 100$ (reported data from May 1st, 2020-July 14th, 2020 [7]). Our findings also confirmed the differences recorded in vi-

ral transmission dynamics globally as our estimates for β_{E0}, β_{I0} and β_{V0} in Tennessee differed from the estimates from Wuhan, China [31, 38].

6.1 RECOMMENDATIONS

There still remain many unanswered questions concerning the SARS CoV-2 virus and its infectious disease which when answered would help the field of mathematical epidemiology in the analytical study and predictions of the transmission dynamics of COVID-19.

Moving forward, we recommend the expansion of this work to evaluate the impact of each awareness program, especially the ongoing vaccination programs globally. Moreover, efforts should be made to track exposed persons as currently, data of individuals in the latent period is not available. Further studies of the model would assess the effect of unavailable means of tracking exposed persons (both symptomatic and asymptomatic) and inadequate testing kits on the transmission dynamics of the coronavirus disease.

Our data fitting results for Tennessee was based on the accumulation of newly infected cases from the set start date, thus accumulated data of infected cases prior to the set date were discarded. This helped in our understanding of the response pattern of awareness programs to newly infected cases. We however hope to include initially accumulated data in future studies of the model.

We also hope to expand this study to better understand the dynamism of the newly discovered COVID-19 variant [43, 44]. Overall, the result of this study imply that applying more strategically created intervention programs based on the viral transmission behavior at a setting can potentially eradicate COVID-19.

REFERENCES

[1] A. S. Amiri, M. Akram, and M. BEMS, "Covid-19: The challenges of the human life," *Social Work & Social Sciences Rewiew*, vol. 17, no. 1, 2020.

[2] W. H. Organization *et al.*, "Statement on the second meeting of the international health regulations (2005) emergency committee regarding the outbreak of novel coronavirus (2019-ncov)," 2005.

[3] P. Anfinrud, V. Stadnytskyi, C. E. Bax, and A. Bax, "Visualizing speech-generated oral fluid droplets with laser light scattering," *New England Journal of Medicine*, vol. 382, no. 21, pp. 2061–2063, 2020.

[4] E. Edwards, "Family clusters: A common pattern for how the coronavirus spreads," *NBC News*, 2020.

[5] D. Lewis, "Mounting evidence suggests coronavirus is airborne—but health advice has not caught up," *Nature*, vol. 583, no. 7817, pp. 510–513, 2020.

[6] W. H. Organization, "WHO Coronavirus Disease (COVID-19) Dashboard." `https://covid19.who.int/`, 2021. [Online; accessed 11-January-2021].

[7] T. S. Government, "TN Novel Coronavirus(COVID-19) Unified command." `https://experience.arcgis.com/experience/885e479b688b4750837ba1d291b85aed`, 2020. [Online; accessed 29-October-2020].

[8] M. D. Knoll and C. Wonodi, "Oxford–astrazeneca covid-19 vaccine efficacy," *The Lancet*, vol. 397, no. 10269, pp. 72–74, 2021.

[9] Bloomberg, "More Than 86.4 Million Shots Given: Covid-19 Tracker." `https://www.bloomberg.com/graphics/covid-vaccine-tracker-global-distribution/`, 2021. [Online; accessed 29-January-2021].

[10] US Food And Drug Administration, "Pfizer-BioNTech COVID-19 Vaccine." `https://www.fda.gov/emergency-preparedness-and-response/coronavirus-disease-2019-covid-19/pfizer-biontech-covid-19-vaccine`, 2021. [Online; accessed 29-January-2021].

[11] CNN, "Chinese Covid-19 vaccine far less effective than initially claimed in Brazil, sparking concerns." `https://www.cnn.com/2021/01/13/asia/sinovac-covid-vaccine-efficacy-intl-hnk/index.html`, 2021. [Online; accessed 29-January-2021].

[12] CNN, "Johnson & Johnson's Covid-19 vaccine, how it works and why it matters." https://www.cnn.com/2021/01/29/health/johnson-covid-19-vaccine-how-it-works/index.html, 2021. [Online; accessed 29-January-2021].

[13] S. R. Dubey, "Corona virus," *International Journal of Nursing Education and Research*, vol. 8, no. 3, pp. 411–414, 2020.

[14] N. Sreenivas, I. Chakarpani, and P. A. Kumar, "The paradigm of entry into host-concerns in developing antivirals for covid-19," *Journal of Interdisciplinary Cycle Research*, 2020.

[15] Z.-W. Ye, S. Yuan, K.-S. Yuen, S.-Y. Fung, C.-P. Chan, and D.-Y. Jin, "Zoonotic origins of human coronaviruses," *International journal of biological sciences*, vol. 16, no. 10, p. 1686, 2020.

[16] C. Liu, Q. Zhou, Y. Li, L. V. Garner, S. P. Watkins, L. J. Carter, J. Smoot, A. C. Gregg, A. D. Daniels, S. Jervey, *et al.*, "Research and development on therapeutic agents and vaccines for covid-19 and related human coronavirus diseases," 2020.

[17] S. Addai, *Mathematical Model of Cerebrospinal Meningitis in Obuasi Municipality of Ashanti Region, Ghana*. PhD thesis, Kwame Nkrumah University of Science and Technology, 2012.

[18] W. O. Kermack and A. G. McKendrick, "A contribution to the mathematical theory of epidemics," *Proceedings of the royal society of london. Series A, Containing papers of a mathematical and physical character*, vol. 115, no. 772, pp. 700–721, 1927.

[19] K. Dietz, "Overall population patterns in the transmission cycle of infectious disease agents," in *Population biology of infectious diseases*, pp. 87–102, Springer, 1982.

[20] F. Wei and R. Xue, "Stability and extinction of seir epidemic models with generalized nonlinear incidence," *Mathematics and Computers in Simulation*, vol. 170, pp. 1–15, 2020.

[21] K. L. Cooke and P. Van Den Driessche, "Analysis of an seirs epidemic model with two delays," *Journal of Mathematical Biology*, vol. 35, no. 2, pp. 240–260, 1996.

[22] A. Turner, C. Jung, P. Tan, S. Gotika, and V. Mago, "A comprehensive model of spread of malaria in humans and mosquitos," in *SoutheastCon 2015*, pp. 1–6, IEEE, 2015.

[23] S. Side, Irwan, U. Mulbar, and W. Sanusi, "Seir model simulation for hepatitis b," in *SEIR model simulation for Hepatitis B*, vol. 1885, p. 020185, 09 2017.

[24] M. Y. Li, J. R. Graef, L. Wang, and J. Karsai, "Global dynamics of a seir model with varying total population size," *Mathematical biosciences*, vol. 160, no. 2, pp. 191–213, 1999.

[25] L. Liu, J. Wang, and X. Liu, "Global stability of an seir epidemic model with age-dependent latency and relapse," *Nonlinear Analysis: real world applications*, vol. 24, pp. 18–35, 2015.

[26] S. J. Weinstein, M. S. Holland, K. E. Rogers, and N. S. Barlow, "Analytic solution of the seir epidemic model via asymptotic approximant," *Physica D: Nonlinear Phenomena*, vol. 411, p. 132633, 2020.

[27] R. K. Upadhyay, A. K. Pal, S. Kumari, and P. Roy, "Dynamics of an seir epidemic model with nonlinear incidence and treatment rates," *Nonlinear Dynamics*, vol. 96, no. 4, pp. 2351–2368, 2019.

[28] G. O. Sabbih, M. A. Korsah, J. Jeevanandam, and M. K. Danquah, "Biophysical analysis of sars-cov-2 transmission and theranostic development via n protein computational characterization," *Biotechnology progress*, p. e3096, 2020.

[29] S. Mandal, T. Bhatnagar, N. Arinaminpathy, A. Agarwal, A. Chowdhury, M. Murhekar, R. R. Gangakhedkar, and S. Sarkar, "Prudent public health intervention strategies to control the coronavirus disease 2019 transmission in india: A mathematical model-based approach," *The Indian journal of medical research*, vol. 151, no. 2-3, p. 190, 2020.

[30] R. Li, S. Pei, B. Chen, Y. Song, T. Zhang, W. Yang, and J. Shaman, "Substantial undocumented infection facilitates the rapid dissemination of novel coronavirus (sars-cov-2)," *Science*, vol. 368, no. 6490, pp. 489–493, 2020.

[31] C. Yang and J. Wang, "A mathematical model for the novel coronavirus epidemic in wuhan, china," *Mathematical biosciences and engineering: MBE*, vol. 17, no. 3, p. 2708, 2020.

[32] R. W. Mbogo and J. W. Odhiambo, "Covid-19 outbreak, social distancing and mass testing in kenya-insights from a mathematical model," *Afrika Matematika*, pp. 1–16, 2021.

[33] H. R. Thieme, "Persistence under relaxed point-dissipativity (with application to an endemic model)," *SIAM Journal on Mathematical Analysis*, vol. 24, no. 2, pp. 407–435, 1993.

[34] D. Gao and S. Ruan, "An sis patch model with variable transmission coefficients," *Mathematical biosciences*, vol. 232, no. 2, pp. 110–115, 2011.

[35] J. LaSalle, "The stability of dynamical systems, regional conf," *Ser. Appl. Math. SIAM, Philadephia*, 1976.

[36] H. C. of Hubei Province, "The Outbreak of New crown Pneumonia in Hubei Province." `http://wjw.hubei.gov.cn/bmdt/dtyw/`, 2019-2020. [Online; accessed 29-September-2020].

[37] T. G. of Wuhan, "The Government of Wuhan homepage." `http://english.wh.gov.cn/`, 2020. [Available Online].

[38] B. Tang, X. Wang, Q. Li, N. L. Bragazzi, S. Tang, Y. Xiao, and J. Wu, "Estimation of the transmission risk of the 2019-ncov and its implication for public health interventions," *Journal of clinical medicine*, vol. 9, no. 2, p. 462, 2020.

[39] J. Spencer, D. P. Shutt, S. K. Moser, H. Clegg, H. J. Wearing, H. Mukundan, and C. A. Manore, "Epidemiological parameter review and comparative dynamics of influenza, respiratory syncytial virus, rhinovirus, human coronavirus, and adenovirus," *MedRxiv*, 2020.

[40] C. Geller, M. Varbanov, and R. E. Duval, "Human coronaviruses: insights into environmental resistance and its influence on the development of new antiseptic strategies," *Viruses*, vol. 4, no. 11, pp. 3044–3068, 2012.

[41] T. D. of Health, "Annual Summaries of Births." `https://www.tn.gov/content/dam/tn/health/documents/vital-statistics/birth/2018/TN\%20Births\%20-\%202018.pdf`, 2018. [Online; accessed 29-October-2020].

[42] T. D. of Health, "Annual Summaries of Deaths." `https://www.tn.gov/content/dam/tn/health/documents/vital-statistics/death/2018/TN\%20Deaths\%20-\%202018.pdf`, 2018. [Online; accessed 29-october-2020].

[43] D. Duong, "What's important to know about the new covid-19 variants?," 2021.

[44] E. Mahase, "Covid-19: What new variants are emerging and how are they being investigated?," 2021.

VITA

Maame Akua Korsah was born in Takoradi, Ghana, to Yaw and Mary Danquah. She completed her primary school education at The Nest School Complex, and her high school education at Archbishop Porter Girls' Senior High School Takoradi, Ghana where she majored in the study of Science. Excelling in mathematics in the West African Certificate Examination after her high school education, she was offered a 1st-degree program in mathematics at the Kwame Nkrumah University of Science and Technology. Due to her hard work, Akua was voted the women's commissioner of the Association of Mathematics and Statistics Students where she worked zealously to promote girl child education. During her undergraduate research project, Akua worked on the topic: Inter-rater agreement between the gynecological diagnosis and pathological evidence on cases of Hysterectomy in Okomfo Anokye Teaching Hospital. She completed her Bachelor of Science degree program in July 2017.

Maame Akua Korsah continued with a teaching internship at Archbishop Porter Girls Senior High School in August 2017 and was voted the women's commissioner of the National Service Personnel Association during her tenure of service. Afterward, she was employed by the Ghana Education Service, where she taught Mathematics at the Takoradi Senior High School. In August 2019, she gained admission into the University of Tennessee at Chattanooga with a graduate teaching assistantship award. Akua is currently working with Professor Jin Wang in the research study of mathematical epidemiology.

Maame Akua Korsah will graduate with a Masters of Science degree in Preprofessional Mathematics in May 2021. Akua will continue her education by pursuing a Ph.D. degree in mathematics. Akua hopes to become a Professor of Mathematics with a genuine interest in mathematical biology.